ORIGINAL ARTICLE

Neuromodulatory effect of vardenafil on aluminium chloride/D-galactose induced Alzheimer's disease in rats: emphasis on amyloid-beta, p-tau, PI3K/Akt/p53 pathway, endoplasmic reticulum stress, and cellular senescence

Heba H. Awad[1] · Mahmoud A. Desouky[2] · Alaa Zidan[3] · Mariam Bassem[3] · Amaal Qasem[3] · Mona Farouk[3] · Haidy AlDeab[3] · Miral Fouad[3] · Cherry Hany[3] · Nada Basem[3] · Rita Nader[3] · Ashrakat Alkalleny[3] · Verina Reda[3] · Mina Y. George[2]

Abstract

Dysregulation of protein homeostasis, proteostasis, is a distinctive hallmark of many neurodegenerative disorders and aging. Deleteriously, the accumulation of aberrant proteins in Alzheimer's disease (AD) is accompanied with a marked collapse in proteostasis network. The current study explored the potential therapeutic effect of vardenafil (VAR), a phosphodiesterase-5 inhibitor, in $AlCl_3$/D-galactose (D-gal)-induced AD in rats and its possible underlying mechanisms. The impact of VAR treatment on neurobehavioral function, hippocampal tissue architecture, and the activity of the cholinergic system main enzymes were assessed utilizing VAR at doses of 0.3 mg/kg and 1 mg/kg. Additionally, the expression level of amyloid-beta and phosphorylated tau proteins in the hippocampus were figured out. Accordingly, VAR higher dose was selected to contemplate the possible underlying mechanisms. Intriguingly, VAR elevated the cyclic guanosine monophosphate level in the hippocampus and averted the repressed proteasome activity by $AlCl_3$/D-gal; hence, VAR might alleviate the burden of toxic protein aggregates in AD. In addition, a substantial reduction in the activating transcription factor 6-mediated endoplasmic reticulum stress was demonstrated with VAR treatment. Notably, VAR counteracted the $AlCl_3$/D-gal-induced depletion of nuclear factor erythroid 2-related factor 2 level. Moreover, the anti-senescence activity of VAR was demonstrated via its ability to restore the balance of the redox circuit. The modulation of phosphatidylinositol-3-kinase/protein kinase B/p53 pathway and the reduction of nuclear factor kappa B level, the key regulator of senescence-associated secretory phenotype mediators release, with VAR treatment were also elucidated. Altogether, these findings insinuate the possible therapeutic benefits of VAR in AD management.

✉ Mina Y. George
  mina.youssif.george@pharma.asu.edu.eg

1   Department of Pharmacology and Toxicology, Faculty of Pharmacy, October University for Modern Sciences and Arts (MSA University), Cairo, Egypt

2   Department of Pharmacology and Toxicology, Faculty of Pharmacy, Ain Shams University, Cairo 11566, Egypt

3   Drug Design Program, Faculty of Pharmacy, Ain Shams University, Cairo, Egypt
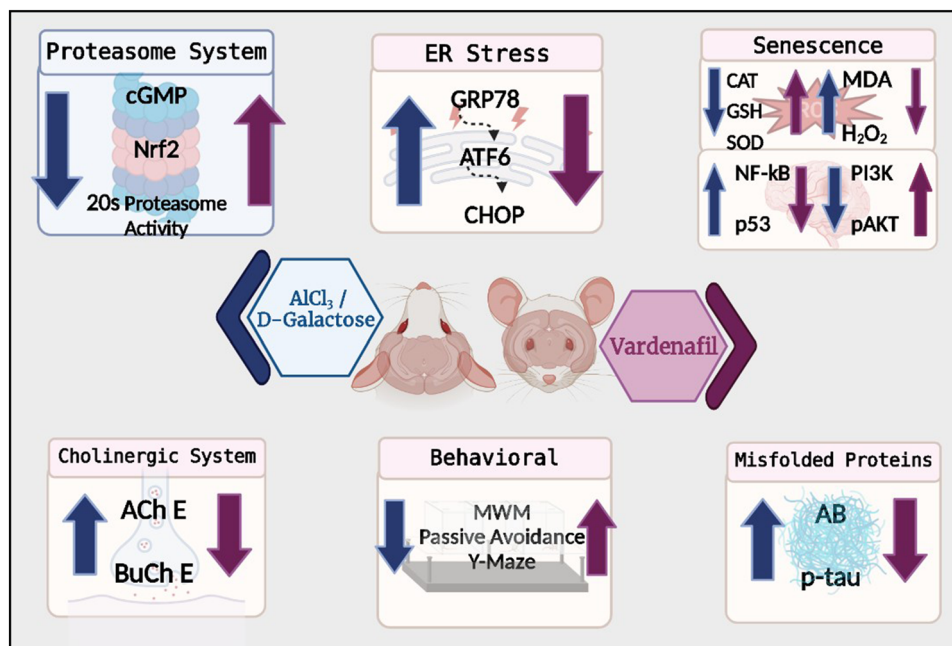
⏣ Springer

Graphic abstract

Introduction

Protein homeostasis, proteostasis, is a pivotal process to maintain the proper balance between newly synthesized proteins and eradication of the misfolded protein species; hence, preserving the stability of the entire proteome (Hipp et al. 2019). Importantly, protein misfolding might occur in 30% of the newly generated proteins and the situation is complicated in neuronal cells, being nondividing cells (Höhn et al. 2020). The two main systems that are implicated in sustaining proteostasis and degradation of misfolded proteins are ubiquitin–proteasome system (UPS) and autophagy (Li et al. 2022). Moreover, the dysregulation of proteostasis network might contribute to proteinopathy (Golde et al. 2013). Several studies indicated that the functional capacity of the proteostasis network is deleteriously affected in many neurodegenerative disorders, such as Alzheimer's disease (AD) in conjunction with aging (Yerbury et al. 2016; Höhn et al. 2020).

AD is a debilitating neurodegenerative disorder characterized by cognitive impairment, as well as marked behavioral alternations, such as depression, apathy, and aggressiveness. Moreover, the aggregation of amyloid-beta (Aβ) and neurofibrillary tangles (NETs) depicts the main pathological features of AD (Silva et al. 2019). Recently, $AlCl_3$/D-galactose (D-gal) combination has been utilized to induce AD in animal models. Interestingly, animals treated with these chemicals have shown a prominent decline in cognitive function, abnormal histological changes in hippocampal tissues, aggregation of AD-associated toxic protein species, and deterioration of the cholinergic system (Zhang et al. 2016b; Haider et al. 2020). Additionally, D-gal has demonstrated a deleterious elevation in several senescence markers inducing senescence in animal models (Hou et al. 2019).

A large body of evidence demonstrated that the catalytic activity of the 26S proteasome, the master of the UPS-related protein degradation, is compromised in AD, resulting in accumulation of misfolded proteins (Thibaudeau et al. 2018; Park et al. 2020). Furthermore, these aggregates might activate endoplasmic reticulum (ER) stressors signals, such as the activating transcription factor 6 (ATF6), generating a cascade of unfolded protein response (UPR). ER stress inducers might also cause a significant elevation in level of C/EBP homologous protein (CHOP), which contributes to cellular demise (Lin et al. 2019; Wang et al. 2020).

Detrimentally, AD is associated with a significant elevation in oxidative stress markers with a notable reduction in nuclear factor erythroid 2-related factor 2 (Nrf2) level (Osama et al. 2020). Conjointly, the phosphatidylinositol 3-kinase (PI3K)/protein kinase B (Akt) cellular pathway was reported to be repressed in senescence models (Zhang et al. 2017). It should be emphasized that significant reduction

in p53 level, a key regulator of cellular apoptosis, might be attributed to Akt-related signals (Chibaya et al. 2021). Additionally, a notable elevation in senescence-associated secretory phenotype (SASP), which includes a vast array of proinflammatory cytokines was elucidated in senescence models (Kumari and Jat 2021).

Vardenafil (VAR), a phosphodiesterase (PDE)-5 inhibitor, is employed for the treatment of erectile dysfunction (Balasubbramanian et al. 2021). Interestingly, the neuroprotective effect of VAR was demonstrated in a subarachnoid hemorrhage rat model (Gul et al. 2010). Also, sildenafil, a PDE-5 inhibitor, alleviated hippocampal damage, neuroinflammation, and modulated the level of phosphorylated Akt (pAkt) in rat model of neonatal hypoxia–ischemia (Yazdani et al. 2021). Collectively, this study aimed at exploring the potential therapeutic effect of VAR in AlCl₃/ᴅ-gal-induced AD model via reinstating normal protein dynamics and its possible anti-senescence actions.

Material and methods

Animals

Male Spargue dawley rats (180 ± 200 g, 8 weeks old) were purchased from Al Roaa Co. for animal breeding, Cairo, Egypt. Rats were left to acclimatize for 14 days before experimentation in an air-conditioned atmosphere (25 °C) with 12 h alternating light and dark cycles. All efforts have been made to minimize animal suffering. Rats were housed in cages with dimensions $80 \times 40 \times 20$ cm³. Animals have free access to food and water ad libitum. Animal food consists of carbohydrates (46.4%), proteins (23.6%), fats (3%), and calcium, phosphorous and fibers (27%).

Drugs and chemicals

VAR was purchased from Bayer Co., for pharmaceutical industries, Cairo, Egypt. AlCl₃ was purchased from Alfa Aesar Co. (Kandel, Germany). ᴅ-gal, Acetylthiocholine iodide, and 5,5′-Dithiobis [2-nitrobenzoic-acid] (DTNB) were purchased from Merck Sigma–Aldrich (St. Louis, MO, USA). For immunohistochemical detection, anti-Aβ and anti-phosphorylated-tau (p-tau) antibody was purchased from ABclonal Technology, MA, US (Catalog No. # A17911 and AP1234, respectively).

Experimental design

A preliminary study was carried out in which thirty-six rats were randomly assigned into six groups (six rats each) and treated for 10 weeks as follows:

Group I (negative control group) received the vehicles daily for 10 weeks. Group II received AlCl₃ (200 mg/kg, oral) and ᴅ-gal (60 mg/kg, i.p.) daily for 10 weeks. Group III received AlCl₃ (200 mg/kg, oral) and ᴅ-gal (60 mg/kg, i.p.) daily for 10 weeks followed by donepezil (1 mg/kg, oral) daily for 5 weeks starting from the sixth week. Groups IV and V rats were treated with AlCl₃ (200 mg/kg, oral) and ᴅ-gal (60 mg/kg, i.p.) daily for 10 weeks. Then, VAR (0.3 mg/kg and 1 mg/kg, oral, respectively) was administered daily starting from the sixth week. Group VI received VAR (1 mg/kg, oral) daily for 5 weeks starting from the sixth week. The doses for AlCl₃, ᴅ-gal, donepezil, and VAR were selected in accordance with previous studies (Akkerman et al. 2014; Chiroma et al. 2019).

Afterwards, rats were subjected to behavioral testing to assess memory functioning as follows: locomotor activity, Morris water maze, step-through passive avoidance, and *y* maze tests. Subsequently, rats were anesthetized, sacrificed by cervical dislocation, skulls were split on ice, and brain tissues were excised. Samples from all groups were fixed in 10% buffered formalin and embedded in paraffin for histological and immunohistochemical examination. Additionally, hippocampi were dissected out and immediately snap frozen in liquid nitrogen and stored at -80 °C for further biochemical analysis.

Based on the results obtained, VAR (1 mg/kg) was selected for further mechanistic investigations. Forty rats were randomly distributed among five groups (eight rats each); Groups I, II, and III were treated as mentioned in the preliminary study. Group IV rats received AlCl₃ (200 mg/kg, oral) and ᴅ-gal (60 mg/kg, i.p.) daily for ten consecutive weeks. Then, VAR (1 mg/kg, oral) was administered daily starting from the sixth week. Group V received VAR (1 mg/kg, oral) daily for 5 weeks starting from the sixth week. Then, rats were sacrificed, brain tissues were excised, and hippocampi from all groups were dissected out and homogenized at 1:10 (w:v) in phosphate-buffered saline (pH = 7.4).

Behavioral assessment

Locomotor activity

The locomotor activity was assessed using Opto-Varimex-Mini Model B, Columbus Instruments, Columbus, OH, USA. Rats' locomotion interrupts IR beams. Locomotor activity was recorded as counts per 5 min (George et al. 2020).

Long-term spatial memory

Morris water maze was carried out using the 5-day test model. A platform was placed at the center of a target quadrant in a-four quadrant circular white pool (Neuroscience,

Osaka, Japan) where its location was kept in changes during the training sessions. Training sessions were performed for five consecutive days for 90 s per rat. On day 5 after the last training session by 3 h, the platform was removed and each rat was placed in the quadrant opposite to the target quadrant and time spent in the target quadrant was monitored and expressed as probe trial (El-Din et al. 2023).

Short term memory

Step-through passive avoidance task was adopted to assess rats' short term memory using Ugo Basile (Italy) apparatus. It is a-two compartment (dark and light) apparatus separated by automatically sliding door. The dark compartment is supplied by an electric current. In the training session, each rat was gently placed in the light compartment and upon entering the dark compartment, the door was closed, an electric shock (0.5 mA–2 s) was conducted, and the cut-off time 90 s. Twenty-four hours later, the testing session (no electric shock) began where rats' latency to step-through to the dark compartment was recorded indicating memory acquisition, (cut-off time = 300 s) (Ayoub et al. 2022).

Short term spatial memory

To perform this task, a *y*-shaped black wooden maze with three similar arms was used. Each rat was placed at the intersecting point of the y maze and left to acclimatize for 5 min. Then, rats' behavior and arm entries for each rat were recorded. Results were expressed as total arm entries (TAE) and spontaneous alternation percentage (SAP) where SAP = [(number of alternations)/(TAE − 2)] × 100 (George et al. 2023).

Histological examination

Using a slide microtome, tissue paraffin blocks were partitioned into 4-µm-thick sections, which were placed on glass slides. After deparaffinization, hematoxylin and eosin staining was conducted and hippocampi from different groups were visualized using Leica Microscope DM500, Wetzlar, Germany (Bancroft and Gamble 2008).

Acetylcholinesterase (AChE) and butyrylcholinesterase (BuChE) activity determination

AChE activity was detected in hippocampi homogenates (Ellman et al. 1961). Briefly, AChE could hydrolyze acetylthiocholine iodide to yield thiocholine, which gives a yellow color in the presence of DTNB detected at 405 nm. Results were expressed as nM/min/gm tissue. BuChE

activity was measured using kit (Catalog No. # CE 1240) purchased from Biodiagnostics, Giza, Egypt. Results were expressed as nM/min/gm tissue.

Immunohistochemical detection of Aβ and p-tau

Following deparaffinization and blocking of 4-µm thickness tissue sections, incubation overnight (4 °C) with both rabbit monoclonal anti-Aβ and rabbit polyclonal anti-p-tau antibodies was performed. Then, biotinylated secondary antibody and streptavidin-HRP were incubated one after the other. Hematoxylin was used for counter staining and the slides were examined using Leica Microscope DM500, Wetzlar, Germany.

Assessment of cyclic guanosine monophosphate (cGMP) level

Quantification of cGMP in hippocampi homogenates was performed using commercial ELISA kit purchased from Biovision, Inc., CA, USA, (Catalog No. # E4717-100). The assay was carried out in accordance with the manufacturer's instructions. Results were expressed as pmol/mg protein.

Proteasome activity determination

A proteasomal activity fluorimetric kit (Cambridge, UK, catalogue No. # ab107921) was used to assess chymotrypsin-like 20S proteasome activity. The intensity of the fluorescence generated from the cleavage of the fluorogenic peptide substrate (Suc-LLVY-AMC) was detected at excitation/emission = 380/460 nm and used as an indicator for proteasomal activity. Results were expressed as RFU/mg protein.

Assessment of ER stress markers

Determination of ATF6, glucose-regulated protein 78 (GRP78), and CHOP levels was carried out using ELISA kits obtained from FineTest, China (Catalogue No. # ER2065), Life span Biosciecnes, Inc., WA (catalogue No. # LS-F38152), and Sunlong Biotech Co, China (Catalogue No. # SL1663Ra), respectively. All procedures were conducted according to the manufacturer's protocol. Results were expressed as pg/mg protein for ATF6 and CHOP and as ng/mg protein for GRP78.

Assessment of Nrf2 level

Nrf2 was determined using ELISA kit purchased from FineTest, China (Catalogue No. # ER962), respectively. All procedures were performed in line with the manufacturer's procedures and results were expressed as pg/mg protein.

Senescence markers determination

Assessment of PI3K, pAkt, and p53 levels

According to the manufacturer's protocol, the hippocampal levels of PI3K, pAkt, and p53 were estimated using commercial ELISA kits purchased from FineTest, China (Catalog No. # ER1837), MyBioSource, San Diego, USA (Catalog No. # MBS7254603), and Cusabio, USA (Catalog No. # CSB-E08336r), respectively.

Assessment of oxidative stress markers

Using kits obtained from kits from Biodiagnostics, Giza, Egypt, redox markers were detected colorimetrically. The

assessment of the antioxidant catalase (CAT) enzyme in the hippocampi of different groups was in accordance with Aebi's method (Aebi 1984). The expression of the enzyme was estimated as unit/mg protein. Moreover, the determination of the reduced glutathione (GSH) level was in consonance with Beutler et al. (1963) and results were expressed as nmol GSH/mg protein. To evaluate the superoxide dismutase (SOD) enzyme activity, its ability to hinder the reduction of nitroblue tetrazolium dye by phenazine methosulphate was used and the color produced was determined at 560 nm over a 5-min period. This method was in agreement with Nishikimi et al. (1972) and results were expressed as U/min/mg protein. Also, according to Aebi (1984) hydrogen peroxide (H_2O_2) was estimated in hippocampal homogenates from various groups and results
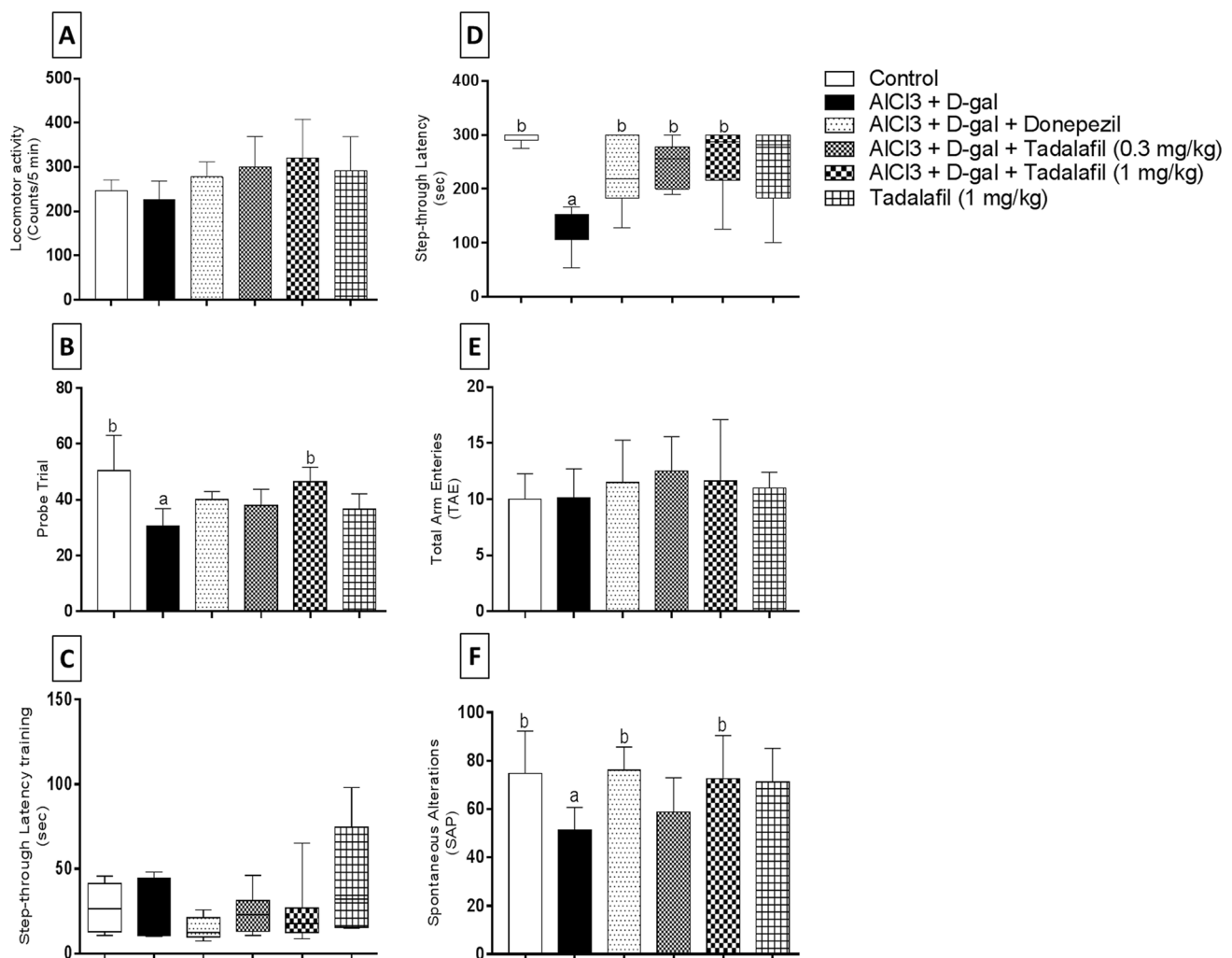
Fig. 1 Effect of vardenafil treatment on locomotor activity test (**A**), probe trial testing (**B**), step-through passive avoidance training (**C**), step-through passive avoidance testing (**D**), total arm entries (**E**), and spontaneous alternations (**F**) against AlCl₃/ᴅ-galactose-induced Alzheimer's disease in rats. Data are presented as mean ± SD ($n = 6$) where: a; statistically significant from control group and b; statistically significant from AlCl₃/ᴅ-galactose-treated group, at $P < 0.05$ using one-way ANOVA followed by Tukey as a post-hoc test (**A**, **B**, **E**, and **F**) and Kruskal–Wallis test followed by Dunn' post hoc test (**C** and **D**)

were expressed as nM/mg protein. Eventually, thiobarbituric acid reactive substances measurement as malondialdehyde (MDA) was employed to evaluate the level of lipid peroxidation in accordance with Kei (1978) and the results were expressed as nmol/mg protein.

Assessment of p105 subunit nuclear factor kappa B (NF-κB) level

The level of hippocampal p105 subunit of NF-κB was determined using ELISA kits obtained from Elab science biotechnology Inc., USA (Catalog No. #E-EL-R0673). Results were expressed as pg/mg protein.

Protein determination

Bradford Protein Assay kit (Catalogue No. #SK3041, Ontario, Canada) was employed to calculate the protein concentration. Briefly, tetradentate copper-protein complexes are generated in an alkaline medium. This complex reduces Folin-Ciocalteu Reagent yielding a water-soluble blue colored product measured at 750 nm.

Statistical analysis

Data were presented as mean $\pm$ SD. The results obtained from passive avoidance test (non-parametric) were analyzed utilizing Kruskal–Wallis test followed by Dunn' as post hoc test. For the rest of data, multiple comparisons were carried out using one-way ANOVA followed by Tukey as a post-hoc test. In all cases, probability values that were less than 0.05 were considered statistically significant. To sketch the graphs, GraphPad Prism software version 8 (GraphPad Software, Inc., La Jolla, CA, USA) was used.

Results

Preliminary study

Behavioral assessment

Locomotor activity One-way ANOVA revealed no significant differences between groups in locomotor activity excluding the effect of locomotion on other behavioral tests (Fig. 1a).
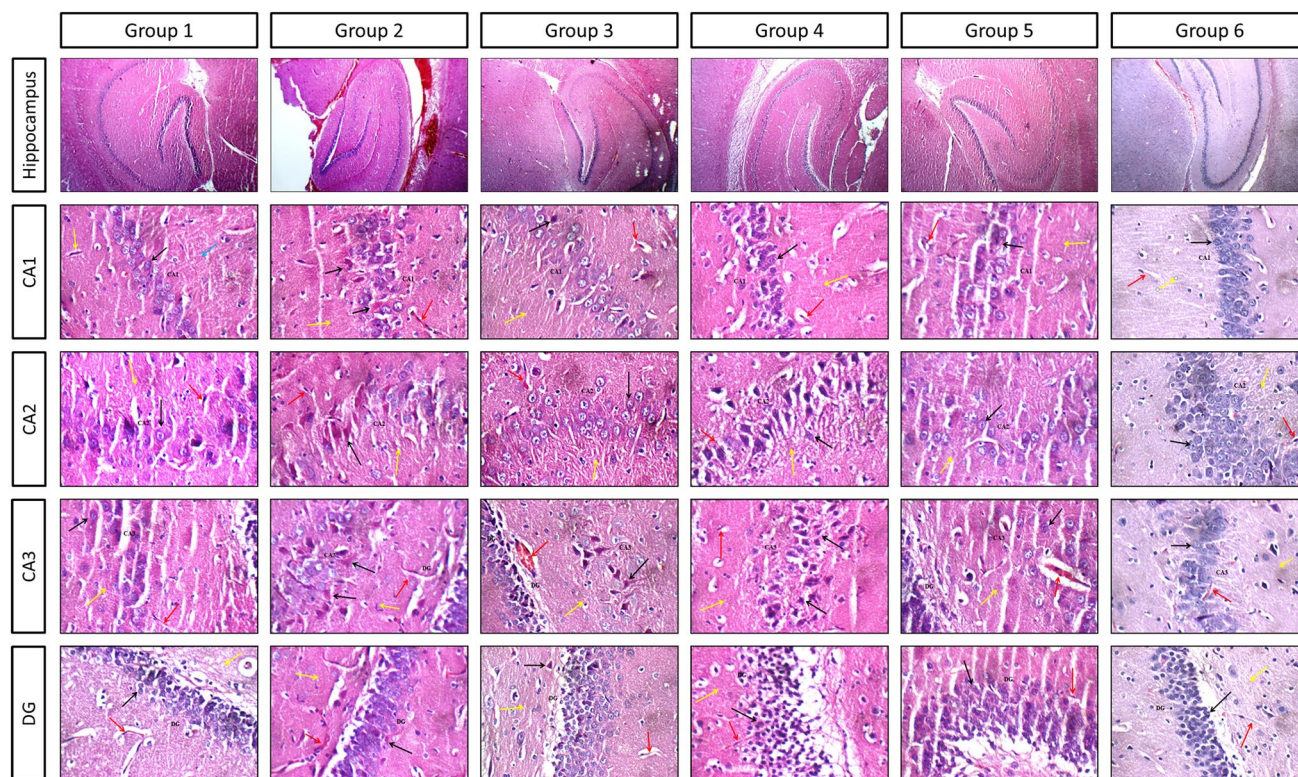
Fig. 2 Effects of vardenafil treatment on AlCl$_3$/D-galactose-induced histological alterations of rat hippocampal CA1, CA2, CA3, and DG regions. Photomicrographs of haematoxylin and eosin-stained sections from control group (group 1); AlCl$_3$/D-galactose-treated group (200 mg/kg, oral) and (60 mg/kg, ip), respectively, (group 2); donepezil-treated group (1 mg/kg) (group 3); vardenafil-treated group (0.3 mg/kg) (group 4); vardenafil-treated group (1 mg/kg) (group 5); vardenafil alone treated group (1 mg/kg) (group 6); with $\times$100 and $\times$200 magnification power

Table 1 Histological changes scoring for hippocampus regions among different groups

| | Hippocampus | | | | | |
| | Pyramidal neurons | | | | Inter-neuron area | Congested blood vessels |
	CA1	CA2	CA3	DG		
Control	0	0	0	0	0	0
AlCl$_3$ (200 mg/kg) + D-gal (60 mg/kg)	+	++	++	+	++	+
AlCl$_3$ + D-gal + Donepezil (1 mg/kg)	+	0	+	+	++	+
AlCl$_3$ + D-gal + VAR (0.3 mg/kg)	0	+	++	0	++	+
AlCl$_3$ + D-gal + VAR (1 mg/kg)	+	0	+	0	0	+
VAR (1 mg/kg)	0	0	0	0	0	0

Effect of VAR and donepezil treatment on Alzheimer's disease induced by AlCl$_3$ and D-galactose in rats. AlCl$_3$ (200 mg/kg, oral) and D-galactose (60 mg/kg, ip) were administered once daily for ten consecutive weeks. Donepezil (1 mg/kg), VAR (0.3 mg/kg), and VAR (1 mg/kg) were administered once daily for 5 consecutive weeks starting from week six. Scorings of histopathological changes were determined in terms of degenerated pyramidal neurons, inter-neuronal area, and congested blood vessels where

0: indicates normal pyramidal neurons, interneuron area, and blood vessels

+: indicates mild degenerated pyramidal neurons, presence of edema in interneuron area, and mildly congested blood vessels

++: indicates markedly degenerated pyramidal neurons, eosinophilic plaque-like area in interneuron areas, and markedly congested blood vessels

Fig. 3 Effect of treatment with vardenafil on hippocampal AChE (**A**) and BuChE activity (**B**) in an experimental model of Alzheimer's disease induced by AlCl$_3$/D-galactose. Data are presented as mean ± SD ($n = 6$) where: a, b, c, and d; statistically significant from control group, AlCl$_3$/D-galactose-treated group, donepezil-treated group, and vardenafil (0.3 mg/kg)-treated group, respectively, at $P < 0.05$ using one-way analysis of variance (ANOVA) followed by Tukey as a post-hoc test
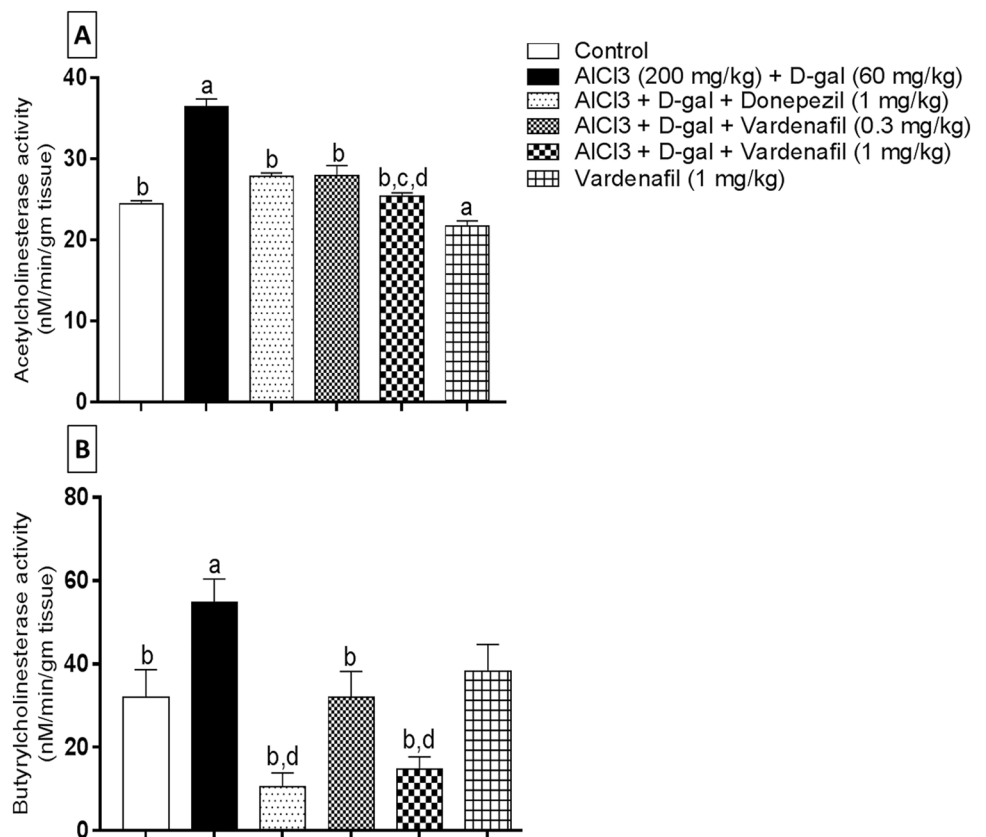
Morris water maze One-way ANOVA showed significant differences between groups in probe trial (Fig. 1b). AlCl$_3$/D-gal treatment caused significant reduction in probe trial by 1.65 folds in comparison with the control group.

Treatment with VAR (1 mg/kg) revealed a statistically significant increase in probe trial by 1.52 folds relative to AlCl$_3$/D-gal-treated group.

Step-through passive avoidance Kruskal–Wallis test revealed no significant differences between groups during the training session (Fig. 1c). Regarding testing session (Fig. 1d), $AlCl_3$/D-gal combination was able to reduce step-through latency by 2.31 folds as compared to the control group. Administration of donepezil, VAR (0.3 mg/kg), and VAR (1 mg/kg) significantly enhanced step-through latency by 1.78, 1.92, 1.92 folds, respectively, against $AlCl_3$/D-gal-induced group.

Y maze There was no significant difference detected regarding TAE (Fig. 1e). However, AD-induced group presented significant reduction in spontaneous alternations relative to the control group by 1.45 folds. Moreover, treatment with either donepezil or VAR (1 mg/kg) illustrated significant increase in spontaneous alternations by 1.48 and 1.41 folds, respectively, as compared to $AlCl_3$/D-gal-treated group (Fig. 1f).

Histological examination

Histological examination for hippocampal regions; CA1, CA2, CA3, and dentate gyrus (DG) is presented in Fig. 2. Control group hippocampi showed normal histological structure for the pyramidal neurons, inter-neuron area, and blood vessels for all regions. Group II hippocampi showed scattered degenerated pyramidal neurons in CA1 and DG regions and markedly degenerated pyramidal neurons with eosinophilic plaque-like areas in CA3 and CA2 regions. In addition, mild congested blood vessels were seen in DG region. Treatment with donepezil presented scattered degenerated pyramidal neurons in CA1, CA3, and DG regions, as well as eosinophilic plaque-like areas in CA1 region. Mild congested blood vessels in DG region were also observed. Treatment with low dose VAR (0.3 mg/kg) revealed scattered degenerated pyramidal neurons in CA2 region, markedly degenerated pyramidal neurons in CA3 region, average
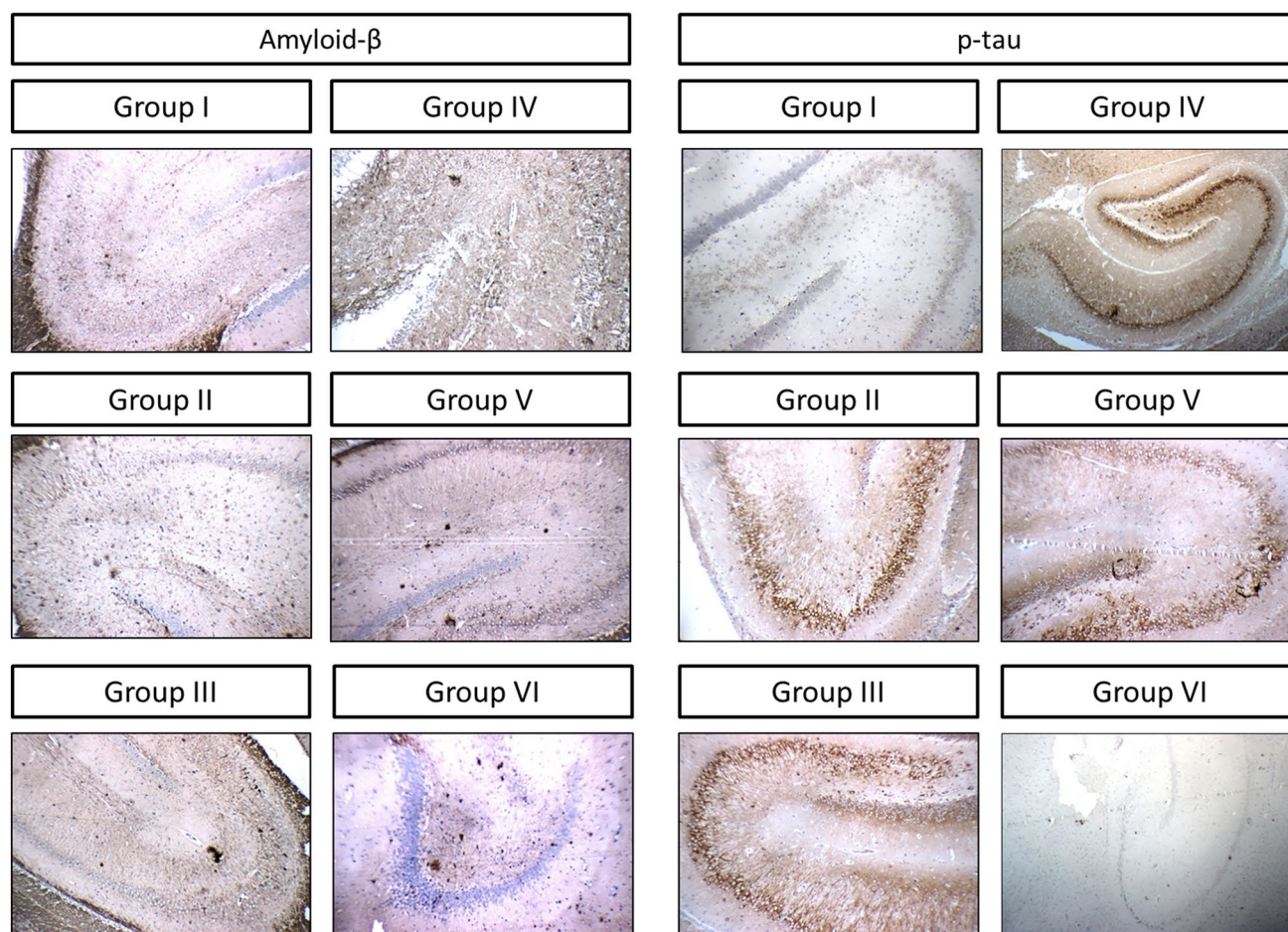
Fig. 4 Expression of the hippocampus amyloid-β and p-tau by immunohistochemical staining (×100). **A** Photomicrographs of histological sections for control group (group I), **B** $AlCl_3$/D-galactose-treated group (200 mg/kg) and (60 mg/kg), respectively (group II), **C** donepezil-treated group (1 mg/kg) (group III), **D** vardenafil-treated group (0.3 mg/kg) (group IV), **E** vardenafil-treated group (1 mg/kg) (group V), and **F** vardenafil alone-treated group (1 mg/kg) (group V). Brown color (positive) indicates specific immunostaining of amyloid-β/p-tau and blue color (negative) indicates hematoxyline staining ($n=3$)

Table 2 Effect of VAR on amyloid-β plaques and p-tau neurofibrillary tangles in AlCl$_3$/D-gal model of AD in rats

Group	Amyloid-β				p-tau			
	CA1	CA2	CA3	DG	CA1	CA2	CA3	DG
Control	–				–			
AlCl$_3$ (200 mg/kg) + D-gal (60 mg/kg)	20.17 ± 4.12[a]				45.5 ± 6.72[a]			
AlCl$_3$ + D-gal + Donepezil (1 mg/kg)	10.5 ± 3.08[b]				26.5 ± 3.01[b,d]			
AlCl$_3$ + D-gal + VAR (0.3 mg/kg)	14.33 ± 2.73[b]				32.17 ± 3.76			
AlCl$_3$ + D-gal + VAR (1 mg/kg)	8.01 ± 2.76[b,d]				20.67 ± 3.67[b,d]			
VAR (1 mg/kg)	–				–			

Effect of VAR (0.3 and 1 mg/kg) treatment on amyloid plaques and p-tau tangles in experimentally induced AD in rats. Data are expressed as mean ± SD ($n = 6$). AlCl$_3$ (200 mg/kg, oral) and D-galactose (60 mg/kg, ip) were administered once daily for ten consecutive weeks. Donepezil (1 mg/kg), VAR (0.3 mg/kg), and VAR (1 mg/kg) were administered once daily for 5 consecutive weeks starting from week six. a, b, and d: significantly different from control group, AlCl$_3$/D-gal-treated group, and AlCl$_3$/D-gal + VAR (0.3 mg/kg)-treated group, respectively, at $P < 0.05$ using one-way ANOVA followed by Tukey as a post-hoc test

inter-neuron areas, and average blood vessels congestion. VAR (1 mg/kg) treatment presented scattered degenerated pyramidal neurons and eosinophilic plaque-like area in CA1 region and mildly congested blood vessels in CA3 region. Group VI showed nearly the same records seen in the control group. Histological scoring is recorded in Table 1.

AChE and BuChE activity

Both enzymes activities were estimated in the hippocampi of different groups. As indicated in Fig. 3, AlCl$_3$/D-gal caused a significant elevation in both AChE (Fig. 3a) and BuChE (Fig. 3b) activities compared to control group by 1.49 and 1.71 folds, respectively. On the other hand, donepezil, VAR (0.3 mg/kg), and VAR (1 mg/kg) treatment promoted the reduction of both enzymes relative to the disease induced group by 1.31, 1.3, and 1.44 folds, respectively, for AChE and by 5.19, 1.71, and 3.73 folds, respectively, for BuChE. Moreover, VAR (1 mg/kg)-treated rats showed significant reduction in AChE activity relative to both donepezil-treated and VAR (0.3 mg/kg)-treated rats by 1.14 and 1.15 folds, respectively. VAR alone-treated group revealed significant reduction in AChE activity compared to the control group by 1.13 folds. Furthermore, donepezil and VAR (1 mg/kg)-treated groups demonstrated significant reduction in BuChE relative to VAR (0.3 mg/kg)-treated group by 3.04 and 2.19 folds, respectively.

Aβ and p-tau expression

Stained Aβ plaques and p-tau NETs (Fig. 4) were counted in the hippocampi of different rats and recorded in Table 2. Regarding Aβ plaques, significant difference was found between normal control group and group II. Additionally, treatment with donepezil, lower VAR dose, and higher VAR dose significantly lowered the number of accumulated plaques relative to the corresponding AlCl$_3$/D-gal-treated group. Interestingly, VAR (1 mg/kg)-treated rats revealed significant reduction in amyloid plaques accumulation relative to the group of rats treated with VAR (0.3 mg/kg) (Suppl. Fig. S1).

Concerning p-tau accumulation, group II revealed significant increase in the number of tangles relative to the corresponding control group. However, significant reduction was detected when comparing donepezil and VAR (1 mg/kg) treated rats with both group II and group IV (Suppl. Fig. S2).

Mechanistic study

cGMP level

The level of cGMP was determined using ELISA technique in hippocampi of different groups to assess its effect on proteasomal activation (Fig. 5a). Data analysis demonstrated that AlCl$_3$/D-gal-treated group showed a detrimental

Fig. 5 Effect of treatment with vardenafil on hippocampal cGMP level (**A**) and 20S proteasome chymotrypsin-like activity (**B**) in an experimental model of Alzheimer's disease induced by $AlCl_3$/D-galactose. Data are presented as mean $\pm$ SD ($n=6$) where: a, b, and c; statistically significant from control group, $AlCl_3$/D-galactose-treated group, and donepezil-treated group, respectively, at $P<0.05$ using one-way analysis of variance (ANOVA) followed by Tukey as a post-hoc test
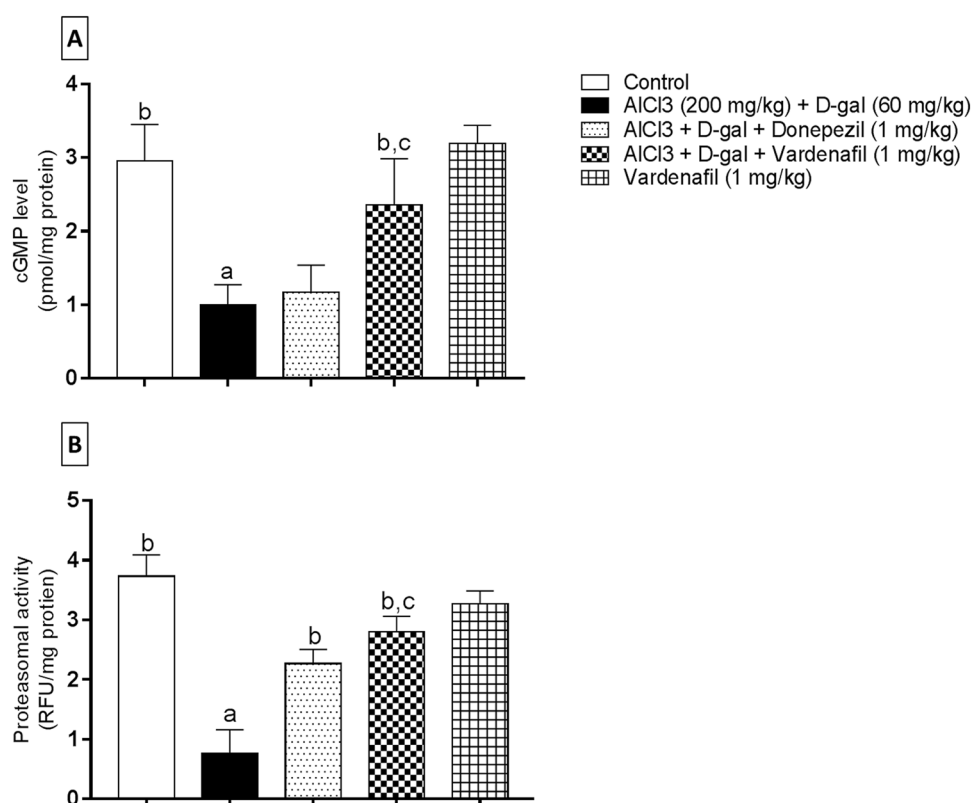
suppression in cGMP level by 2.97 compared to the control group. VAR treatment was significantly able to oppose this effect, resulting in a dominant amplification of cGMP levels by 2.36 and 2.01 folds when compared to $AlCl_3$/D-gal and donepezil-treated group, respectively.

Proteasomal activity

As evident from Fig. 5b, $AlCl_3$/D-gal-treated rats exhibited a significant decrease in chymotrypsin-like activity by 4.88 folds relative to the control group. Treatment with either donepezil or VAR was able to reverse such effect in a significant manner compared to the disease-induced group by 2.96 and 3.67 folds, respectively. Interestingly, upon VAR co-administration, the proteasomal activity to degrade the Suc-LLVY-AMC substrate was significantly enhanced by 1.24 folds contrary to donepezil-treated group.

ER stress markers

As illustrated in Fig. 6a, initial hippocampal GRP78 level was significantly elevated in group II rats by 1.36 folds when compared to the control group. While administration of VAR (1 mg/kg) effectively abrogated GRP78 level by 1.28 folds relative to $AlCl_3$/D-gal-treated group. VAR alone-treated rats showed significant elevation in GRP78 level by 1.29 folds relative to the corresponding control group. Afterwards, as

shown in Fig. 6b, ATF6 level was found to be significantly elevated in the $AlCl_3$/D-gal-treated group by 1.48 folds relative to the control group. On the other side, donepezil and VAR treatment inhibited ATF6 level by 1.34 and 1.39 folds, respectively, in comparison to the disease-induced group. Additionally, one-way ANOVA showed significant augmentation in CHOP level following $AlCl_3$/D-gal treatment by 1.24 folds relative to the control group. On the contrary, oral administration of VAR showed marked inhibition in CHOP level by 1.17 folds relative to the group II rats (Fig. 6c).

Nrf2 level

The effect of PDE-5 inhibition on Nrf2 level in hippocampi of the different groups was investigated (Fig. 6d). It was found that Nrf2 level in group II was significantly suppressed by 1.92 folds when compared to the control group. Besides, donepezil and VAR (1 mg/kg) treatment significantly enhanced the level Nrf2 by 2.23 and 1.93 folds, respectively, relative to the $AlCl_3$/D-gal-treated group.

Senescence markers

PI3K/pAkt/p53 pathway markers

Firstly, hippocampal PI3K level was assessed in different groups (Fig. 7a). Data analysis revealed significant reduction
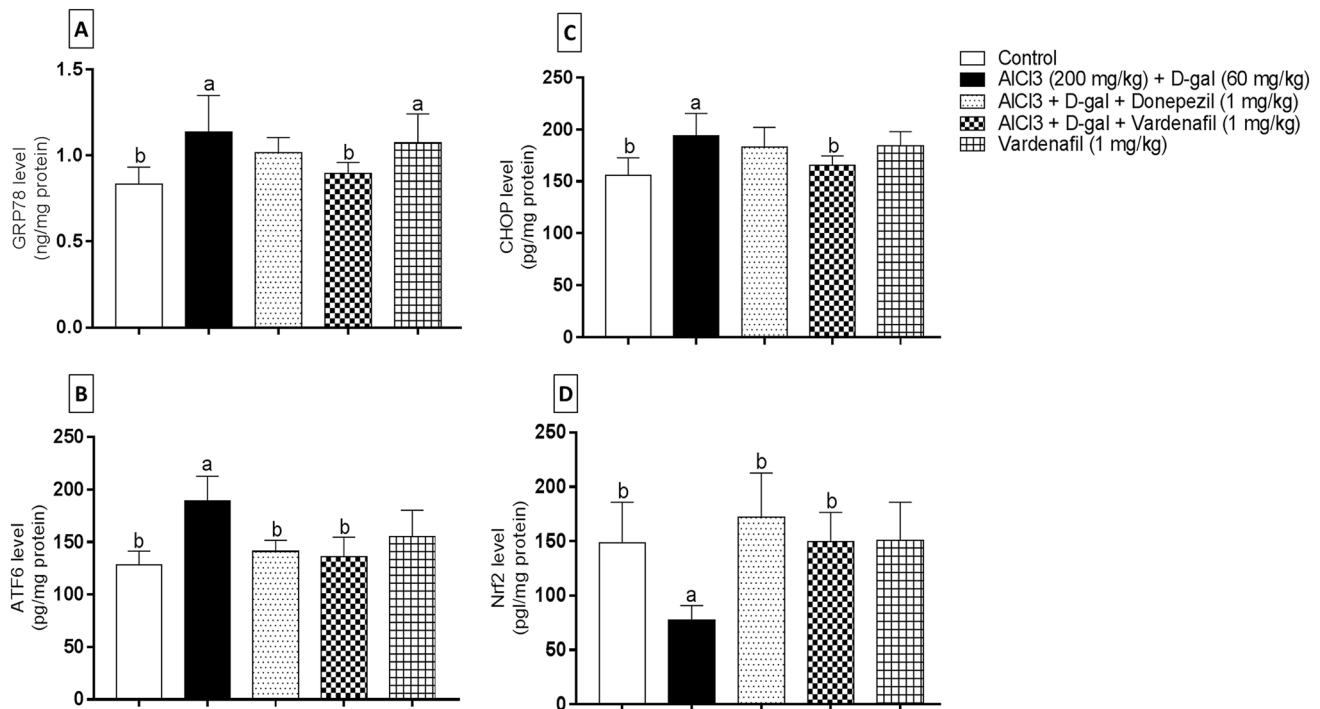
Fig. 6 Effect of treatment with vardenafil treatment on hippocampal GRP78 (**A**), ATF6 (**B**), CHOP (**C**), and Nrf2 (**D**) in an experimental model of Alzheimer's disease induced by AlCl$_3$/D-galactose. Data are presented as mean $\pm$ SD ($n = 6$) where: a and b; statistically significant from control group and AlCl$_3$/D-galactose-treated group, respectively, at $P < 0.05$ using one-way analysis of variance (ANOVA) followed by Tukey as a post-hoc test

in AlCl$_3$/D-gal-treated rats compared to the control group by 1.47 folds. On the other side, VAR treatment showed significant elevation in PI3K level by 1.52 folds relative to AlCl$_3$/D-gal-treated group.

Moreover, pAkt level was found to be reduced significantly in hippocampus of group II rats when compared to the control group by 1.42 folds. Moreover, hippocampal pAkt was enhanced in a significant manner following VAR (1 mg/kg) treatment relative to group II rats by 1.36 folds (Fig. 7b).

Finally, the apoptotic p53 level was measured in the hippocampi of different groups (Fig. 7c). A 1.56-fold significant increase was detected in AlCl$_3$/D-gal-treated group relative to the control group. By contrast, group of rats treated with VAR showed significant reduction by 1.23 folds compared to disease induced group.

Oxidative stress markers

The levels of CAT, GSH, SOD, MDA, and H$_2$O$_2$ were assessed in the hippocampi of different treatment groups (Fig. 8). First of all, significant reduction in CAT level was found in AlCl$_3$/D-gal-treated group relative to the corresponding control group by 1.21 folds. However, donepezil and VAR treatment opposed this reduction and showed

significant elevation in CAT level relative to the disease-induced group by 1.24 and 1.22 folds, respectively (Fig. 8a).

Secondarily, AlCl$_3$/D-gal-treated group illustrated a significant reduction by 1.34 folds in GSH level as compared to the control group. Interestingly, treatment with either donepezil or VAR significantly elevated GSH level compared group II rats by 1.33 and 1.38 folds, respectively (Fig. 8b).

Moreover, regarding SOD activity (Fig. 8c), group II rats showed reduced hippocampal SOD activity in a significant manner compared to the control group by 3.01 folds. On the other hand, donepezil and VAR treatment opposed this reduction and enhanced SOD activity significantly relative to AlCl$_3$/D-gal-treated rats by 3.42 and 3.02 folds, respectively.

Furthermore, lipid peroxidation level determined as MDA was found to be significantly elevated by 2.24 folds in AlCl$_3$/D-gal-treated rats compared to the control group. Interestingly, VAR administration was found to reduce MDA level compared to both group II and donepezil-treated rats in a significant manner by 1.74 and 2.21 folds, respectively (Fig. 8d).

Finally, H$_2$O$_2$ level was further assessed and one-way ANOVA results revealed an insignificant elevation in H$_2$O$_2$ in AlCl$_3$/D-gal-intoxicated rats relative to the corresponding control group. However, a significant reduction in H$_2$O$_2$ level
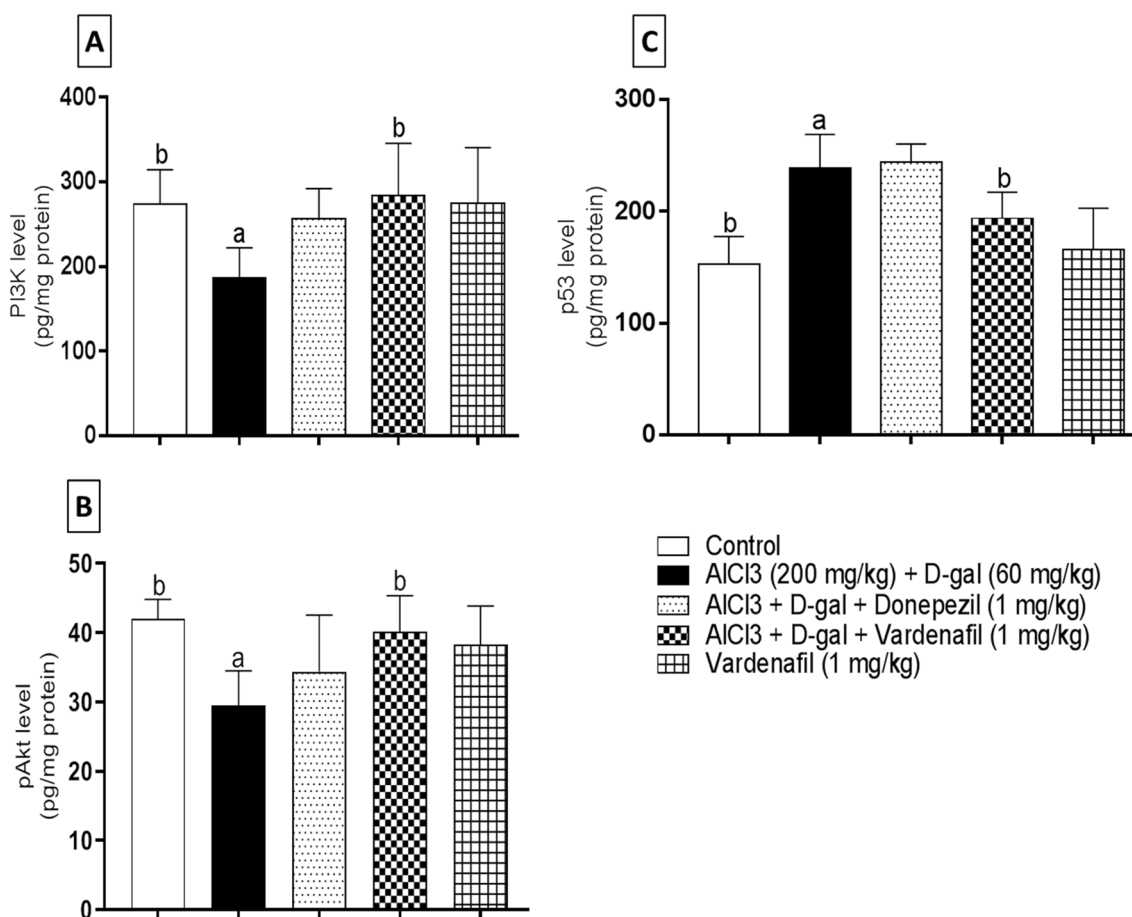
Fig. 7 Effect of treatment with vardenafil on hippocampal PI3K (**A**), pAkt (**B**), and p53 (**C**) in an experimental model of Alzheimer's disease induced by AlCl₃/ᴅ-galactose. Data are presented as mean ± SD (*n* = 6) where: a and b; statistically significant from control group and AlCl₃/ᴅ-galactose-treated group, respectively, at $P < 0.05$ using one-way analysis of variance (ANOVA) followed by Tukey as a post-hoc test

was found following VAR administration relative to group II rats by 1.54 folds (Fig. 8e).

p105 subunit NF-κB level

As illustrated in Fig. 8f, AlCl₃/ᴅ-gal-treated group of rats revealed significant increase in p105 subunit of NF-κB relative to the control group by 1.59 folds. By contrast, a significant reduction of 1.53 and 1.69 folds was shown when comparing donepezil and VAR (1 mg/kg) treated rats, respectively, to the AD-induced group of rats.

Discussion

Proteostasis depicts a pivotal cellular process guarantees that properly folded proteins are produced and misfolded proteins are eliminated (Hipp et al. 2019). Normal eukaryotic cells possess an interconnected network known as protein quality control systems, which thoroughly check cellular proteins and detect any fault in their folding to be directed for protein degradation systems (Chen et al. 2011). Interestingly, this surveillance task is mainly attributed to UPS, which is mainly concerned with the elimination of many dysfunctional short-lived proteins linked to ubiquitin (Ub) molecules, as well as autophagy that breakdowns the long-lived proteins (Kocaturk and Gozuacik 2018). Accordingly, any lapse in this ramified network might compromise its integrity, leading to the accumulation of aggregation-prone proteins (Hipp et al. 2019). It is well-established that the capacity of the UPS system is dampened in multiple neurodegenerative disorders and aging (Zheng et al. 2016; Graham and Liu 2017). Scholars have pointed out that misfolded proteins can detrimentally impair the principal degradation mechanisms of the UPS system, resulting in further aggregation of toxic protein species, which collectively creates a vicious cycle wobbles between the collapse of the UPS and proteinopathy (Farizatto et al. 2017; Thibaudeau et al. 2018). To this end, promoting the activity of the UPS might bring a new
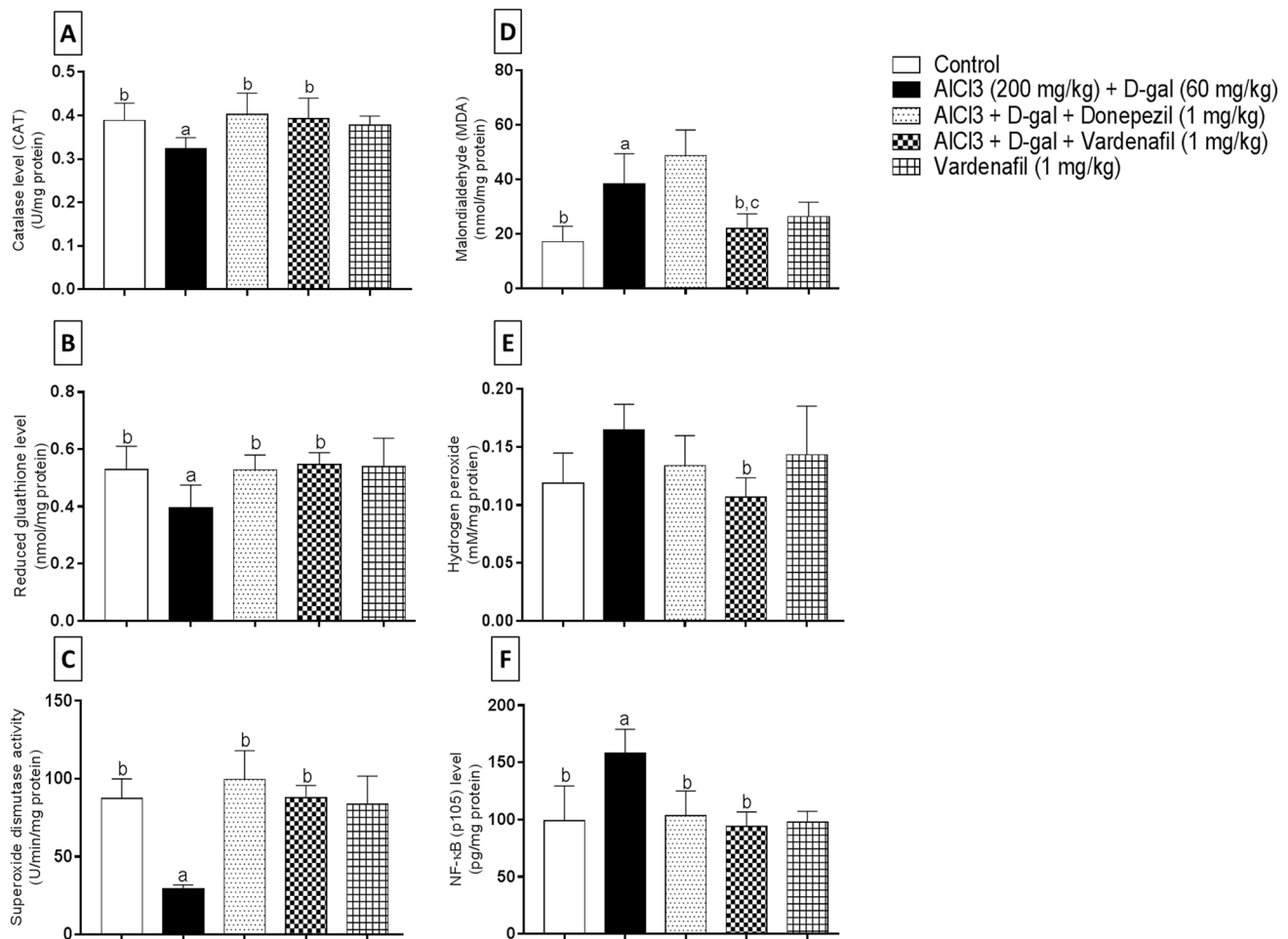
Fig. 8 Effect of treatment with vardenafil on hippocampal catalase (**A**), reduced glutathione (**B**), superoxide dismutase activity (**C**), malondialdehyde (**D**), hydrogen peroxide (**E**), and p105 subunit of NF-κB (**F**) in an experimental model of Alzheimer's disease induced by AlCl₃/ᴅ-galactose. Data are presented as mean ± SD ($n = 6$) where: a, b, and c; statistically significant from control, AlCl₃/ᴅ-galactose-treated group, and donepezil-treated group, respectively, at $P < 0.05$ using one-way analysis of variance (ANOVA) followed by Tukey as a post-hoc test

hope in many neurodegenerative diseases and proteotoxic disorders (Njomen and Tepe 2019).

Basically, AD is a devastating neurodegenerative disorder, which constitutes 60–80% of all cases of dementia. Accumulation of amyloid plaques and NETs are the main pathological features of AD (Abubakar et al. 2022). The amyloidogenic Aβ, a well-known player in amyloid plaques, is generated from Aβ-precursor protein by β-secretases and γ-secretases enzymes while NET might arise from the hyperphosphorylation of tau protein (Knopman et al. 2021; Abubakar et al. 2022).

A growing body of evidence suggests that elevated brain burden of AlCl₃ could be associated with excessive free radical production, cognitive impairment, and attenuation in the cholinergic system functionality in the hippocampus; hence, it mimics the pathological features of AD (Singh et al. 2018). Importantly, continuous exposure to AlCl₃ leads to

the appearance of Aβ aggregates and NFT alongside with the development of significant oxidative damage and ER stress (Ahmad Rather et al. 2019; Promyo et al. 2020). Recently, ᴅ-gal has been identified as a potential chemical that can be utilized to evoke aging via elevating the advanced glycation end product and reactive oxygen species (ROS) production (Rahman et al. 2022). Furthermore, ᴅ-gal hinders neurogenesis in the hippocampus with a marked cognitive impairment; thereby, it represents an effective substrate to study aging in animal models (Nam et al. 2019). Consequently, administration of AlCl₃/ᴅ-gal elicited a notable biochemical and behavioral changes that are similar to human AD pathophysiology and thus constitutes a robust AD model (Wei et al. 2017; Chiroma et al. 2018).

To investigate the potential therapeutic impacts of PDE-5 inhibitor, VAR, in alleviating the burden of toxic agglomerates; a preliminary study was firstly conducted to determine

the VAR optimal therapeutic dose in our AD model. Importantly, donepezil, was used in this study as a standard treatment for AD to solidify our hypothesis (Haider et al. 2020). Initially, cognitive deficits and memory impairment were observed with rats intoxicated with AlCl$_3$/D-gal, which was consistent with previous studies (Haider et al. 2020; Liu et al. 2022). Curiously, VAR enhanced memory, learning abilities, and cognition. This improvement in the neurobehavioral function with VAR high dose treatment was evidenced by increasing the time spent in the target quadrant in Morris water maze, escalation of step-through latency, and improved spontaneous alternations in y maze test. It is worthy to mention that VAR higher dose showed superior results concerning long-term spatial memory (Morris water maze) and short-term spatial memory (y maze) relative to the lower dose. Relevantly, tadalafil, PDE-5 inhibitor, treatment resulted in a marked improvement in memory in a rat model of hyperhomocysteinemia induced vascular dementia (Bhatia and Singh 2022).

Secondarily, histopathological examination of CA1, CA2, CA3, and DG hippocampal regions was thoroughly performed. Normal histological architecture was observed in control and drug alone groups. Expectedly, exposure to AlCl$_3$/D-gal caused a substantial neurodegeneration, loss of neuronal organized arrangement, congested blood vessels, and apoptotic alternations in various hippocampal regions, which was in accordance with previous study utilized this combination to induce AD (Gao et al. 2022). Contradictorily, co-treatment with VAR high dose restored nearly the original neuronal architecture and mitigated the number of degenerated neurons while the VAR low dose mildly alleviated the AlCl$_3$/D-gal-induced neurodegeneration. Interestingly, these results were supported by an earlier study proved that cilostazol, PDE-3 inhibitor, abrogated the histological anomalies in AD rat model (Khalifa et al. 2022).

Furthermore, several studies explored the role AChE and BuChE enzymes as critical nodes of the cholinergic system dysfunction in AD. The level of these enzymes is notably increased in AD patients; consequently, agents that can inhibit these enzymes might unveil valuable approach in AD treatment (Mushtaq et al. 2014). Strikingly, co-ingestion of VAR and donepezil counteracted the considerable elevation in the activity of both AChE and BuChE enzymes that was induced by AlCl$_3$/D-gal. It is worthy to mention that VAR (1 mg/kg) showed powerful results concerning AChE and BuChE relative to the lower dose (0.3 mg/kg). Interestingly, VAR higher dose administration revealed more AChE inhibition relative to donepezil treatment while they showed nearly same results regarding BuChE activity. The significant reduction in AChE activity was in accordance with Haider et al. (2020).

To consolidate the potential therapeutic effect of VAR high dose, the expression level of the main AD pathological hallmarks was explored. In line with previously documented, the expression level of the toxic protein species, Aβ and p-tau, was markedly boosted with AlCl$_3$/D-gal treatment in the hippocampus (Zhang et al. 2016b). However, co-administration of VAR and donepezil abrogated the expression level of Aβ and p-tau NETs, which support the hypothesis that alleviation of misfolded proteins burden might be attributed to the activation of UPS (Goldberg et al. 2021). In our study, both donepezil and VAR high dose demonstrated superior results concerning p-tau deposition than lower VAR dose. Additionally, Aβ deposition was found to be markedly decreased following VAR (1 mg/kg) than VAR (0.3 mg/kg) treatment.

Based on the previous results obtained from the preliminary study regarding; neurobehavioral tests, histological examination, AChE and BuChE activities, Aβ expression, and p-tau accumulation results, VAR high dose was selected to demonstrate the mechanistic study.

In the heart of the UPS system is the 26S proteasome (~ 2.5 MDa), which represent the executive arm for UPS-mediated misfolded protein degradation (Kaake et al. 2014). Basically, it is a barrel shaped complex that comprises 20S core particle with one or two 19S regulatory particles located at the end of the 20S core. The 20S particle has four heteroheptameric rings assembled together and composed of seven α-subunits, as well as seven β-subunits. Importantly, the β1, β2, and β5 subunits house a substantial caspase-like, trypsin-like, and chymotrypsin-like activity, respectively, that can degrade the Ub-tagged proteins (Kaake et al. 2014; Livneh et al. 2016).

As previously mentioned, the catalytic capacity of the 26S proteasome is surmounted in several proteotoxic disorders and with aging; thus, enhancing the proteasome activity might reveal a bright spot in the management of many neurodegenerative diseases such as AD (Graham and Liu 2017; Thibaudeau et al. 2018). In line with this, this study sheds the light on how proteasome capacity could be activated through the elevation of cGMP level. cGMP is a distinctive secondary messenger that is produced in a variety of cells and tissues. Moreover, cGMP generation is catalyzed via the activation of soluble guanylyl cyclase after its binding with nitric oxide or particulate guanylyl cyclase enzyme as a consequence of its activation with the natriuretic peptides (Friebe et al. 2020). Protein kinase G (PKG) is one of the fundamental effectors of cGMP, which plays a pivotal role in many cellular functions (Francis et al. 2010; Friebe et al. 2020). Consistently, VAR was utilized in this study. Rats intoxicated with AlCl$_3$/D-gal showed a marked reduction in cGMP level, which was consistent with a previous study reported that the hippocampal level of cGMP could be reduced in AD with a deleterious alternations in memory (Hesse et al. 2017); however, a clear boost in the cGMP level was demonstrated in the hippocampi of VAR-treated

animals. Pertinently, recent studies highlighted the potential impact of vericiguat, soluble guanylyl cyclase activator, in memory acquisition and augmenting hippocampal plasticity in rats (Nelissen et al. 2021).

Furthermore, to consolidate the potential impact of VAR against aggregation-prone proteins in AD, the 20S catalytic activity was evaluated via chymotrypsin-like activity fluorimetric assay. Expectedly, AD-associated misfolded protein aggregates were associated a considerable reduction in the 20S peptidase activity, which comes in agreement with Thibaudeau et al. (2018). Contradictorily, VAR adequately augmented the degradation capacity of the 20S core particle. Also, VAR treatment showed superior results compared to donepezil-treated rats. Such alleviation of the burden of aberrant proteins might be attributed to the upregulated level of cGMP, which activates PKG. Furthermore, cGMP-PKG regulatory circuit activation intensifies the 20S capacity to degrade toxic protein species (VerPlank et al. 2020). Likewise, cAMP-PKA pathway activation was previously reported to broaden the 20S peptidase activity via the phosphorylation of Rpn6 proteasome subunit (Lokireddy et al. 2015). Distinctively, the exact site of phosphorylation of the 26S subunits by PKG protein is still not concluded (VerPlank et al. 2020). Concertedly, these results suggest that restoring the activity of the UPS system and mitigating the level of Aβ and NET misfolded proteins after VAR treatment might delineate unconventional paradigm for AD treatment.

ER is a cardinal cellular organelle implicated in protein quality control via its ability to control precise protein folding and post-translational modifications (Araki and Nagata 2011; Adams et al. 2019a). Importantly, a large body of evidence indicated that accumulation of misfolded protein plaques in many neurodegenerative disorders results in the development of ER stress (Sprenkle et al. 2017; Ghemrawi and Khair 2020). To restore the original protein balance, cells initiate a cascade known as UPR, which is transduced via three transmembrane sensor proteins: double-stranded RNA dependent protein kinase-like ER kinase, inositol-requiring enzyme-1α, and ATF6 (Sprenkle et al. 2017; Adams et al. 2019b).

During normal cellular conditions, these stress detectors anchor themselves to a well-known ER chaperone protein, GRP78, which prevent their activation. However, during stressful conditions, such as misfolded protein burden, they free GRP78 away from the transmembrane sensors allowing UPR signal activation (Zhu and Lee 2015; Bartoszewska and Collawn 2020). ATF6 becomes liberated from the ER to enter the Golgi apparatus. Afterwards, ATF6 is translocated into the nucleus adjusting the expression of many targeted genes involved in protein folding (Chiang et al. 2019). Additionally, sustained ER stress contributes to cellular death (Sano and Reed 2013; Ghemrawi and Khair 2020). CHOP is pro-apoptotic factor with an extremely low level of

expression; however, under ER stress conditions the ATF6 arm upregulate CHOP expression (Li et al. 2014; Moriguchi et al. 2019). CHOP itself is tangled with the modulation of expression of several anti-apoptotic and pro-apoptotic genes leading to apoptosis (Li et al. 2014; Hu et al. 2019).

Recently, it is widely accepted that ER stress is a key player in AD as figured out from the postmortem brain tissues of AD patients. Similarly, several ER stress markers were showed to be detrimentally elevated in AD, which can be correlated with Aβ-induced ER stress (Uddin et al. 2020). Additionally, marked alternations in the levels of ER molecular chaperones and folding enzymes are documented with aging (Brown and Naidoo 2012). Likewise, rats received AlCl₃/ᴅ-gal displayed a meaningful ER stress as evidenced by the significant rise in GRP78, ATF6, and CHOP levels as previously reported in rat model of ᴅ-gal-induced aging (Dai et al. 2023). VAR properly halted the levels of these ER stress key biomarkers. This VAR-associated ER stress alleviation could be ascribed to the elevation of proteasome activity that led to a notable amelioration of neurotoxic proteins and finally buffering the ER stress. As far as we can tell that this is the first study that revealed novel avenues in treating AlCl₃/ᴅ-gal-induced AD via restoring proteostasis and dampening the ER stress. Moreover, donepezil treatment did not show any significance change concerning the levels of GRP78 and CHOP relative to AlCl₃/ᴅ-gal-treated rats.

Dysfunction of the redox state is one of the classical features of AD and aging (Holubiec et al. 2022; Rahman et al. 2022). It is worth noting that our brain is highly susceptible to the imbalance of this regulatory circuit owing to its attenuated antioxidants safeguards and inherit high rate of oxygen utilization. Deleteriously, mitochondrial damage and elevated level of ROS in AD compromise the capacity of antioxidant enzymes (Cenini et al. 2019). Nrf2 is an essential transcription factor that act as a defensive guard against oxidative stress owing to its ability to regulate the expression of several antioxidant genes (Yang et al. 2021). Primarily, under normal physiological conditions, Nrf2 is arrested into the cytoplasm, ubiquitinated, and degraded via proteasomal-mediated process though during stressful cellular events, Nrf2 enters the nucleus, where it can bind to antioxidant responsive element to trigger many protective pathways (Gugliandolo et al. 2020). Previous studies revealed that Nrf2 is greatly affected in wide array of neurodegenerative disorders, including AD (Cuadrado 2016). A large body of evidence reported that, Nrf2 deficiency might result in a profound increment in senescence markers, neuro-inflammation, and oxidative stress in addition to proteinopathy (Cuadrado 2016; Fulop et al. 2018). Interestingly, an earlier study demonstrated that activating Nrf2 might be an effective strategy to attenuate ᴅ-gal-prompted neurotoxicity and memory impairment (Sun et al. 2020).

Consonantly, our model showed a notable reduction in hippocampal Nrf2 nuclear fraction after AlCl$_3$/D-gal treatment as previously reported (Liu et al. 2022). Alternatively, VAR co-treatment abrogated the reduction of Nrf2 nuclear translocation, which might reveal a striking potential anti-aging activity. Donepezil treatment revealed nearly the same results as VAR. Intriguingly, Nrf2 is implicated in the regulation of expression of several proteasome subunits and a striking enhancement in the proteasome capacity was revealed with Nrf2 enhancers (Kwak et al. 2003; Pajares et al. 2017).

PI3K/Akt signaling circuit, is one of the most pivotal cellular cascades being involved in wide range of neuronal functions, such as survival, neurogenesis, and apoptosis (Long et al. 2021). Recently, a deleterious repression of PI3K/Akt axis in AD was reported. Moreover, restoration of the activity of this pathway, ameliorated Aβ-induced neurotoxicity (Zhang et al. 2016a). Interestingly, AlCl$_3$/D-gal treatment depicted a detrimental suppression of PI3k and pAkt levels as previously reported (Li et al. 2016). Consistently, our study revealed that VAR co-treatment abrogated AlCl$_3$/D-gal inhibitory effect on PI3K/Akt pathway, which comes in agreement with a previous study denoted that tadalafil might activate PI3K/Akt signaling cascade (Lee et al. 2021). Donepezil treatment showed insignificant change relative to AlCl$_3$/D-gal treatment.

Importantly, p53 is one of the well-established senescence-associated markers owning to its ability to orchestrate many downstream targets that regulate cell cycle arrest and apoptosis (Mijit et al. 2020). Our study demonstrated that rats treated with AlCl$_3$/D-gal showed a marked elevation in p53 level. Relevantly, upregulation of p53 protein level was highlighted in D-gal-induced senescence model (Sha et al. 2021). VAR treatment halted the p53 elevated level; thus, our study augmented a recent study indicated that Akt might act as a negative regulator of p53 (Chibaya et al. 2021). Donepezil showed no effect on p53 hippocampal level. Additionally, PI3K/Akt signaling cascade might be involved in the detoxification of ROS via regulating the activity of Nrf2 transcription factor (Xu et al. 2022).

The anti-senescence activity of VAR was also emphasized via its ability to buffer oxidative stress in the hippocampus. In the present study, AlCl$_3$/D-gal-induced oxidative stress was evidenced by CAT and GSH low levels, as well as low enzymatic activity of SOD; however, lipid peroxidation MDA level was notably elevated in hippocampi of the diseased group. Intriguingly, this deleterious oxidative stress was consistent with previous reports that used AlCl$_3$/D-gal combination (Wei et al. 2017; Liu et al. 2022). Notable reduction in oxidative stress was substantiated with VAR co-administration as it promoted the level of CAT and GSH with a marked escalation of SOD enzyme activity. The antioxidant power of VAR was further confirmed via its ability to dampen the levels of MDA and H$_2$O$_2$, which suggests an additional defensive line against oxidative stress in AD and accelerated aging. It is worthy to mention that VAR treatment revealed significant superior results concerning MDA and H$_2$O$_2$ compared to donepezil treatment. These results solidified a previous study showed the potential antioxidant activity of VAR (El-Agamy et al. 2018). Curiously, VAR capability to relieve oxidative stress might be a direct consequence of Nrf2 pathway activation and enhanced expression of cytoprotective machineries (Francisqueti-Ferron et al. 2019). Additionally, our results were in consonance with a previous study, which documented that cGMP-PKG circuit might be considered a key activator of Nrf2 (Yu et al. 2018).

A large body of evidence showed that senescence is characterized with a selective cellular phenotype, SASP. Moreover, SASPs classical components encompass wide range of proinflammatory cytokines, matrix metalloproteinases, and various proteases (Kumari and Jat 2021). Mounting evidence has revealed that multiple SASP biomarkers are elevated in AD different models (Dorigatti et al. 2022). One of the key regulators of SASP is NF-κB, which orchestrates gene expression of several pro-inflammatory mediators (Kumari and Jat 2021). Concordantly, our study figured out a substantial elevation in the level of NF-κB p105 subunit in the diseased rats as previously mentioned in Song et al. (Song et al. 2022). Contradictorily, VAR mitigated the level of NF-κB 105 subunit; thus, VAR anti-senescence effect might be a direct cause of its ability to inhibit the release of downstream pro-inflammatory mediators of NF-κB. Donepezil treatment showed nearly similar results as VAR. Additionally, triggering ER stress via ATF6 axis represents a crucial arm in cellular senescence (Kim et al. 2019); thus, ER stress mitigation via VAR treatment might present a possible interpretation for VAR anti-senescence action.

Exposure to AlCl$_3$ might induce a deleterious cognitive impairment, hippocampal neurodegeneration, cholinergic dysfunction, and accumulation of amyloid plaques (Chen et al. 2021). Once reached the brain of rats, AlCl$_3$ deteriorates axonal transport, long-term potentiation, resulting in profound neurodegeneration (Liaquat et al. 2017). Unfortunately, one of the molecular and pathological limitations of this model is the pathological difference between AD-associated plaques in human and the chemically generated plaques in rats (Rapaka et al. 2022). Also, there was no clinical evidence reported linking AlCl$_3$ to the development of AD in humans. Additionally, D-gal administration causes marked pathological changes that mimic the human brain aging process as well as, induction of cholinergic dysfunction; thus, can be used to study the molecular mechanisms of AD (Mahdi et al. 2021).

However, ᴅ-gal is a sugar and might affect blood glucose level especially with chronic exposure. This may occur via its ability to instigate insulin resistance state (Akhtar et al. 2022; Rapaka et al. 2022). Collectively, ᴅ-gal could mimic natural aging process and AlCl₃ induces neurodegeneration, thus, their co-administration may result in pathological changes that could mimic AD features. Currently, no AD experimental model can entirely mimic human AD pathophysiology; however, knowing the limitations of each model might bring a new hope in battle against this leading neurodegenerative disorder (Blaikie et al. 2022).

Conclusions

In conclusion, the current study emphasized the potential therapeutic effect of VAR in AlCl₃/ᴅ-gal-induced AD. VAR co-treatment successfully dampened memory deficits and histological anomalies in the hippocampus. Moreover, to the best of the authors' knowledge, this is the first study, which elucidated the proteasomal modulatory effect of VAR in AlCl₃/ᴅ-gal-induced AD via activation of cGMP-PKG regulatory circuit. Also, significant reduction in ER stress was revealed with VAR treatment. VAR attenuated the Nrf2 depletion and activated the PI3K/Akt pathway. Finally, VAR alleviated oxidative stress and mitigated the key SASP modulator, NF-κB p105 subunit. Hence, VAR repurposing might unveil a previously unseen approach in treating age-related neurological disorders via restoring normal dynamics of various protein quality control systems.

Declarations

References

Abubakar MB, Sanusi KO, Ugusman A, Mohamed W, Kamal H, Ibrahim NH, Khoo CS, Kumar J (2022) Alzheimer's disease: an update and insights into pathophysiology. Front Aging Neurosci 14:742408. https://doi.org/10.3389/fnagi.2022.742408

Adams BM, Oster ME, Hebert DN (2019a) Protein quality control in the endoplasmic reticulum. Protein J 38(3):317–329. https://doi.org/10.1007/s10930-019-09831-w

Adams CJ, Kopp MC, Larburu N, Nowak PR, Ali MMU (2019b) Structure and molecular mechanism of ER stress signaling by the unfolded protein response signal activator IRE1. Front Mol Biosci 6:11. https://doi.org/10.3389/fmolb.2019.00011

Aebi H (1984) Catalase in vitro. Methods Enzymol 105:121–126. https://doi.org/10.1016/s0076-6879(84)05016-3

Ahmad Rather M, Justin-Thenmozhi A, Manivasagam T, Saravanababu C, Guillemin GJ, Essa MM (2019) Asiatic acid attenuated aluminum chloride-induced tau pathology, oxidative stress and apoptosis via AKT/GSK-3β signaling pathway in wistar rats. Neurotox Res 35(4):955–968. https://doi.org/10.1007/s12640-019-9999-2

Akhtar A, Gupta SM, Dwivedi S, Kumar D, Shaikh MF, Negi A (2022) Preclinical models for Alzheimer's disease: past, present, and future approaches. ACS Omega 7(51):47504–47517. https://doi.org/10.1021/acsomega.2c05609

Akkerman S, Prickaerts J, Bruder AK, Wolfs KH, De Vry J, Vanmierlo T, Blokland A (2014) PDE5 inhibition improves object memory in standard housed rats but not in rats housed in an enriched

environment: Implications for memory models? PLoS ONE 9(11):e111692. https://doi.org/10.1371/journal.pone.0111692

Araki K, Nagata K (2011) Protein folding and quality control in the ER. Cold Spring Harbor Perspect Biol 3(11):a007526. https://doi.org/10.1101/cshperspect.a007526

Ayoub IM, George MY, Menze ET, Mahmoud M, Botros M, Essam M, Ashmawy I, Shendi P, Hany A, Galal M, Ayman M, Labib RM (2022) Insights into the neuroprotective effects of *Salvia officinalis* L. and *Salvia microphylla* Kunth in the memory impairment rat model. Food Funct 13(4):2253–2268. https://doi.org/10.1039/d1fo02988f

Balasubbramanian D, Dharani S, Tauseef M, Khan MA, Rahman Z, Mitchell BM (2021) High dose vardenafil blunts the hypertensive effects of toll-like receptor 3 activation during pregnancy. Front Virol 1:2021. https://doi.org/10.3389/fviro.2021.780298

Bancroft JD, Gamble M (2008) Theory and practice of histological techniques. Elsevier, London

Bartoszewska S, Collawn JF (2020) Unfolded protein response (UPR) integrated signaling networks determine cell fate during hypoxia. Cell Mol Biol Lett 25(1):18. https://doi.org/10.1186/s11658-020-00212-1

Beutler E, Duron O, Kelly BM (1963) Improved method for the determination of blood glutathione. J Lab Clin Med 61:882–888

Bhatia P, Singh N (2022) Tadalafil ameliorates memory deficits, oxidative stress, endothelial dysfunction and neuropathological changes in rat model of hyperhomocysteinemia induced vascular dementia. Int J Neurosci 132(4):384–396. https://doi.org/10.1080/00207454.2020.1817009

Blaikie L, Kay G, Maciel P, Kong Thoo Lin P (2022) Experimental modelling of Alzheimer's disease for therapeutic screening. Eur J Med Chem Rep 5:100044. https://doi.org/10.1016/j.ejmcr.2022.100044

Brown MK, Naidoo N (2012) The endoplasmic reticulum stress response in aging and age-related diseases. Front Physiol 3:263. https://doi.org/10.3389/fphys.2012.00263

Cenini G, Lloret A, Cascella R (2019) Oxidative stress in neurodegenerative diseases: from a mitochondrial point of view. Oxid Med Cell Longev 2019:2105607. https://doi.org/10.1155/2019/2105607

Chen B, Retzlaff M, Roos T, Frydman J (2011) Cellular strategies of protein quality control. Cold Spring Harbor Perspect Biol 3(8):a004374. https://doi.org/10.1101/cshperspect.a004374

Chen X, Zhang M, Ahmed M, Surapaneni KM, Veeraraghavan VP, Arulselvan P (2021) Neuroprotective effects of ononin against the aluminium chloride-induced Alzheimer's disease in rats. Saudi J Biol Sci 28(8):4232–4239. https://doi.org/10.1016/j.sjbs.2021.06.031

Chiang WJ, Kroeger H, Chea L, Lin JH (2019) Pathomechanisms of ATF6-associated cone photoreceptor diseases. Adv Exp Med Biol 1185:305–310. https://doi.org/10.1007/978-3-030-27378-1_50

Chibaya L, Karim B, Zhang H, Jones SN (2021) Mdm2 phosphorylation by Akt regulates the p53 response to oxidative stress to promote cell proliferation and tumorigenesis. Proc Natl Acad Sci USA. https://doi.org/10.1073/pnas.2003193118

Chiroma SM, Mohd Moklas MA, Mat Taib CN, Baharuldin MTH, Amon Z (2018) d-Galactose and aluminium chloride induced rat model with cognitive impairments. Biomed Pharmacother 103:1602–1608. https://doi.org/10.1016/j.biopha.2018.04.152

Chiroma SM, Hidayat Baharuldin MT, Mat Taib CN, Amom Z, Jagadeesan S, Adenan MI, Mohd Moklas MA (2019) Protective effect of *Centella asiatica* against (ᴅ)-galactose and aluminium chloride induced rats: behavioral and ultrastructural approaches. Biomed Pharmacother 109:853–864. https://doi.org/10.1016/j.biopha.2018.10.111

Cuadrado A (2016) NRF2 in neurodegenerative diseases. Curr Opin Toxicol 1:46–53. https://doi.org/10.1016/j.cotox.2016.09.004

Dai XJ, Jia Y, Cao R, Zhou MN (2023) Naringin prevents cognitive dysfunction in aging rats by inhibiting toll-like receptor 4 (TLR4)/NF-κB pathway and endoplasmic reticulum stress. Evid Based Complement Altern Med Ecam 2023:2919811. https://doi.org/10.1155/2023/2919811

Dorigatti AO, Riordan R, Yu Z, Ross G, Wang R, Reynolds-Lallement N, Magnusson K, Galvan V, Perez VI (2022) Brain cellular senescence in mouse models of Alzheimer's disease. Geroscience 44(2):1157–1168. https://doi.org/10.1007/s11357-022-00531-5

El-Agamy DS, Almaramhy HH, Ahmed N, Bojan B, Alrohily WD, Elkablawy MA (2018) Anti-inflammatory effects of vardenafil against cholestatic liver damage in mice: a mechanistic study. Cell Physiol Biochem Int J Exp Cell Physiol Biochem Pharmacol 47(2):523–534. https://doi.org/10.1159/000489986

El-Din MIG, George MY, Youssef FS (2023) Chemical characterization of the polyphenolic rich fraction of *Thunbergia erecta* and its therapeutic potential against doxorubicin and cyclophosphamide-induced cognitive impairment in rats. J Ethnopharmacol 307:116213. https://doi.org/10.1016/j.jep.2023.116213

Ellman GL, Courtney KD, Andres V Jr, Feather-Stone RM (1961) A new and rapid colorimetric determination of acetylcholinesterase activity. Biochem Pharmacol 7:88–95. https://doi.org/10.1016/0006-2952(61)90145-9

Farizatto KLG, Ikonne US, Almeida MF, Ferrari MFR, Bahr BA (2017) Aβ42-mediated proteasome inhibition and associated tau pathology in hippocampus are governed by a lysosomal response involving cathepsin B: evidence for protective crosstalk between protein clearance pathways. PLoS ONE 12(8):e0182895. https://doi.org/10.1371/journal.pone.0182895

Francis SH, Busch JL, Corbin JD, Sibley D (2010) cGMP-dependent protein kinases and cGMP phosphodiesterases in nitric oxide and cGMP action. Pharmacol Rev 62(3):525–563. https://doi.org/10.1124/pr.110.002907

Francisqueti-Ferron FV, Ferron AJT, Garcia JL, Silva C, Costa MR, Gregolin CS, Moreto F, Ferreira ALA, Minatel IO, Correa CR (2019) Basic concepts on the role of nuclear factor erythroid-derived 2-like 2 (Nrf2) in age-related diseases. Int J Mol Sci. https://doi.org/10.3390/ijms20133208

Friebe A, Sandner P, Schmidtko A (2020) cGMP: a unique 2nd messenger molecule—recent developments in cGMP research and development. Naunyn Schmiedebergs Arch Pharmacol 393(2):287–302. https://doi.org/10.1007/s00210-019-01779-z

Fulop G, Kiss T, Tarantini S, Balasubramanian P, Yabluchanskiy A, Farkas E, Bari F, Ungvari Z, Csiszar A (2018) Nrf2 deficiency in aged mice exacerbates cellular senescence promoting cerebrovascular inflammation. GeroScience. https://doi.org/10.1007/s11357-018-0047-6

Gao D, Li P, Gao F, Feng Y, Li X, Li D, Li Y, Xiao Y (2022) Preparation and multitarget anti-AD activity study of chondroitin sulfate lithium in AD mice induced by combination of D-Gal/AlCl(3). Oxid Med Cell Longev 2022:9466166. https://doi.org/10.1155/2022/9466166

George MY, Menze ET, Esmat A, Tadros MG, El-Demerdash E (2020) Potential therapeutic antipsychotic effects of Naringin against ketamine-induced deficits in rats: involvement of Akt/GSK-3β and Wnt/β-catenin signaling pathways. Life Sci 249:117535. https://doi.org/10.1016/j.lfs.2020.117535

George MY, El-Derany MO, Ahmed Y, Zaher M, Ibrahim C, Waleed H, Khaled H, Khaled G, Saleh A, Alshafei H, Alshafei R, Ahmed N, Ezz S, Ashraf N, Ibrahim SS (2023) Design and evaluation of chrysin-loaded nanoemulsion against lithium/pilocarpine-induced status epilepticus in rats; emphasis on formulation, neuronal excitotoxicity, oxidative stress, microglia polarization, and AMPK/SIRT-1/PGC-1α pathway. Expert

Opin Drug Deliv 20(1):159–174. https://doi.org/10.1080/17425247.2023.2153831

Ghemrawi R, Khair M (2020) Endoplasmic reticulum stress and unfolded protein response in neurodegenerative diseases. Int J Mol Sci. https://doi.org/10.3390/ijms21176127

Goldberg AL, Kim HT, Lee D, Collins GA (2021) Mechanisms that activate 26S proteasomes and enhance protein degradation. Biomolecules. https://doi.org/10.3390/biom11060779

Golde TE, Borchelt DR, Giasson BI, Lewis J (2013) Thinking laterally about neurodegenerative proteinopathies. J Clin Investig 123(5):1847–1855. https://doi.org/10.1172/jci66029

Graham SH, Liu H (2017) Life and death in the trash heap: the ubiquitin proteasome pathway and UCHL1 in brain aging, neurodegenerative disease and cerebral Ischemia. Ageing Res Rev 34:30–38. https://doi.org/10.1016/j.arr.2016.09.011

Gugliandolo A, Bramanti P, Mazzon E (2020) Activation of Nrf2 by natural bioactive compounds: A promising approach for stroke? Int J Mol Sci. https://doi.org/10.3390/ijms21144875

Gul S, Bahadir B, Hanci V, Bektas S, Can M, Kalayci M, Acikgoz S, Acikgoz B (2010) Effect of vardenafil on cerebral vasospasm following experimental subarachnoid hemorrhage in rats. J Clin Neurosci off J Neurosurg Soc Aust 17(8):1038–1041. https://doi.org/10.1016/j.jocn.2010.02.001

Haider S, Liaquat L, Ahmad S, Batool Z, Siddiqui RA, Tabassum S, Shahzad S, Rafiq S, Naz N (2020) Naringenin protects AlCl3/ᴅ-galactose induced neurotoxicity in rat model of AD via attenuation of acetylcholinesterase levels and inhibition of oxidative stress. PLoS ONE 15(1):e0227631. https://doi.org/10.1371/journal.pone.0227631

Hesse R, Lausser L, Gummert P, Schmid F, Wahler A, Schnack C, Kroker KS, Otto M, Tumani H, Kestler HA, Rosenbrock H, von Arnim CAF (2017) Reduced cGMP levels in CSF of AD patients correlate with severity of dementia and current depression. Alzheimer's Res Ther 9(1):17. https://doi.org/10.1186/s13195-017-0245-y

Hipp MS, Kasturi P, Hartl FU (2019) The proteostasis network and its decline in ageing. Nat Rev Mol Cell Biol 20(7):421–435. https://doi.org/10.1038/s41580-019-0101-y

Höhn A, Tramutola A, Cascella R (2020) Proteostasis failure in neurodegenerative diseases: focus on oxidative stress. Oxid Med Cell Longev 2020:5497046. https://doi.org/10.1155/2020/5497046

Holubiec MI, Gellert M, Hanschmann EM (2022) Redox signaling and metabolism in Alzheimer's disease. Front Aging Neurosci 14:1003721. https://doi.org/10.3389/fnagi.2022.1003721

Hou J, Yun Y, Xue J, Sun M, Kim S (2019) ᴅ-Galactose induces astrocytic aging and contributes to astrocytoma progression and chemoresistance via cellular senescence. Mol Med Rep 20(5):4111–4118. https://doi.org/10.3892/mmr.2019.10677

Hu H, Peng L, Jiang H, Shen H, Zhou P, Gao Y (2019) Silenced CHOP protects pancreatic B-cell function by targeting peroxisome proliferator-activated receptor-γ coactivator-1α through nuclear factor-κB signaling pathway in diabetes mellitus. J Cell Biochem 120(8):12595–12603. https://doi.org/10.1002/jcb.28526

Kaake RM, Kao A, Yu C, Huang L (2014) Characterizing the dynamics of proteasome complexes by proteomics approaches. Antioxid Redox Signal 21(17):2444–2456. https://doi.org/10.1089/ars.2013.5815

Kei S (1978) Serum lipid peroxide in cerebrovascular disorders determined by a new colorimetric method. Clin Chim Acta 90(1):37–43. https://doi.org/10.1016/0009-8981(78)90081-5

Khalifa M, Abdelsalam RM, Safar MM, Zaki HF (2022) Phosphodiesterase (PDE) III inhibitor, Cilostazol, improved memory impairment in aluminum chloride-treated rats: modulation of cAMP/CREB pathway. Inflammopharmacology 30(6):2477–2488. https://doi.org/10.1007/s10787-022-01010-1

Kim HS, Kim Y, Lim MJ, Park YG, Park SI, Sohn J (2019) The p38-activated ER stress-ATF6α axis mediates cellular senescence. FASEB J off Publ Feder Am Soc Exp Biol 33(2):2422–2434. https://doi.org/10.1096/fj.201800836R

Knopman DS, Amieva H, Petersen RC, Chételat G, Holtzman DM, Hyman BT, Nixon RA, Jones DT (2021) Alzheimer disease. Nat Rev Dis Prime 7(1):33. https://doi.org/10.1038/s41572-021-00269-y

Kocaturk NM, Gozuacik D (2018) Crosstalk between mammalian autophagy and the ubiquitin-proteasome system. Front Cell Dev Biol 6:128. https://doi.org/10.3389/fcell.2018.00128

Kumari R, Jat P (2021) Mechanisms of cellular senescence: cell cycle arrest and senescence associated secretory phenotype. Front Cell Dev Biol 9:645593. https://doi.org/10.3389/fcell.2021.645593

Kwak MK, Wakabayashi N, Greenlaw JL, Yamamoto M, Kensler TW (2003) Antioxidants enhance mammalian proteasome expression through the Keap1-Nrf2 signaling pathway. Mol Cell Biol 23(23):8786–8794. https://doi.org/10.1128/mcb.23.23.8786-8794.2003

Lee WC, Leu S, Wu KLH, Tain YL, Chuang YC, Chan JYH (2021) Tadalafil ameliorates bladder overactivity by restoring insulin-activated detrusor relaxation via the bladder mucosal IRS/PI3K/AKT/eNOS pathway in fructose-fed rats. Sci Rep 11(1):8202. https://doi.org/10.1038/s41598-021-87505-3

Li Y, Guo Y, Tang J, Jiang J, Chen Z (2014) New insights into the roles of CHOP-induced apoptosis in ER stress. Acta Biochim Biophys Sin 46(8):629–640. https://doi.org/10.1093/abbs/gmu048

Li H, Kang T, Qi B, Kong L, Jiao Y, Cao Y, Zhang J, Yang J (2016) Neuroprotective effects of ginseng protein on PI3K/Akt signaling pathway in the hippocampus of ᴅ-galactose/AlCl3 inducing rats model of Alzheimer's disease. J Ethnopharmacol 179:162–169. https://doi.org/10.1016/j.jep.2015.12.020

Li Y, Li S, Wu H (2022) Ubiquitination-proteasome system (UPS) and autophagy two main protein degradation machineries in response to cell stress. Cells. https://doi.org/10.3390/cells11050851

Liaquat L, Ahmad S, Sadir S, Batool Z, Khaliq S, Tabassum S, Emad S, Madiha S, Shahzad S, Haider S (2017) Development of AD like symptoms following co-administration of AlCl3 and D-gal in rats: a neurochemical, biochemical and behavioural study. Pak J Pharm Sci 30(2(Suppl.)):647–653

Lin L, Liu G, Yang L (2019) Crocin improves cognitive behavior in rats with Alzheimer's disease by regulating endoplasmic reticulum stress and apoptosis. Biomed Res Int 2019:9454913. https://doi.org/10.1155/2019/9454913

Liu Y, Meng X, Sun L, Pei K, Chen L, Zhang S, Hu M (2022) Protective effects of hydroxy-α-sanshool from the pericarp of *Zanthoxylum bungeanum* Maxim. On ᴅ-galactose/AlCl₃-induced Alzheimer's disease-like mice via Nrf2/HO-1 signaling pathways. Eur J Pharmacol 914:17691. https://doi.org/10.1016/j.ejphar.2021.174691

Livneh I, Cohen-Kaplan V, Cohen-Rosenzweig C, Avni N, Ciechanover A (2016) The life cycle of the 26S proteasome: from birth, through regulation and function, and onto its death. Cell Res 26(8):869–885. https://doi.org/10.1038/cr.2016.86

Lokireddy S, Kukushkin NV, Goldberg AL (2015) cAMP-induced phosphorylation of 26S proteasomes on Rpn6/PSMD11 enhances their activity and the degradation of misfolded proteins. Proc Natl Acad Sci USA 112(52):E7176-7185. https://doi.org/10.1073/pnas.1522332112

Long HZ, Cheng Y, Zhou ZW, Luo HY, Wen DD, Gao LC (2021) PI3K/AKT signal pathway: a target of natural products in the prevention and treatment of Alzheimer's disease and Parkinson's disease. Front Pharmacol 12:648636. https://doi.org/10.3389/fphar.2021.648636

Mahdi O, Chiroma SM, Hidayat Baharuldin MT, Mohd Nor NH, Mat Taib CN, Jagadeesan S, Devi S, Mohd Moklas MA (2021) WIN55,212–2 attenuates cognitive impairments in AlCl$_3$ + d-galactose-induced Alzheimer's disease rats by enhancing neurogenesis and reversing oxidative stress. Biomedicines 9(9):1270

Mijit M, Caracciolo V, Melillo A, Amicarelli F, Giordano A (2020) Role of p53 in the regulation of cellular senescence. Biomolecules. https://doi.org/10.3390/biom10030420

Moriguchi M, Watanabe T, Fujimuro M (2019) Capsaicin induces ATF4 translation with upregulation of CHOP, GADD34 and PUMA. Biol Pharm Bull 42(8):1428–1432. https://doi.org/10.1248/bpb.b19-00303

Mushtaq G, Greig NH, Khan JA, Kamal MA (2014) Status of acetylcholinesterase and butyrylcholinesterase in Alzheimer's disease and type 2 diabetes mellitus. CNS Neurol Disord Drug Targets 13(8):1432–1439. https://doi.org/10.2174/1871527313666141023141545

Nam SM, Seo M, Seo JS, Rhim H, Nahm SS, Cho IH, Chang BJ, Kim HJ, Choi SH, Nah SY (2019) Ascorbic acid mitigates d-galactose-induced brain aging by increasing hippocampal neurogenesis and improving memory function. Nutrients. https://doi.org/10.3390/nu11010176

Nelissen E, Argyrousi EK, Van Goethem NP, Zhao F, Hines CDG, Swaminath G, Gerisch M, Hueser J, Sandner P, Prickaerts J (2021) Soluble guanylate cyclase stimulator vericiguat enhances long-term memory in rats without altering cerebral blood volume. Biomedicines. https://doi.org/10.3390/biomedicines9081047

Nishikimi M, Appaji N, Yagi K (1972) The occurrence of superoxide anion in the reaction of reduced phenazine methosulfate and molecular oxygen. Biochem Biophys Res Commun 46(2):849–854. https://doi.org/10.1016/s0006-291x(72)80218-3

Njomen E, Tepe JJ (2019) Proteasome activation as a new therapeutic approach to target proteotoxic disorders. J Med Chem 62(14):6469–6481. https://doi.org/10.1021/acs.jmedchem.9b00101

Osama A, Zhang J, Yao J, Yao X, Fang J (2020) Nrf2: a dark horse in Alzheimer's disease treatment. Ageing Res Rev 64:101206. https://doi.org/10.1016/j.arr.2020.101206

Pajares M, Cuadrado A, Rojo AI (2017) Modulation of proteostasis by transcription factor NRF2 and impact in neurodegenerative diseases. Redox Biol 11:543–553. https://doi.org/10.1016/j.redox.2017.01.006

Park J, Cho J, Song EJ (2020) Ubiquitin-proteasome system (UPS) as a target for anticancer treatment. Arch Pharmacal Res 43(11):1144–1161. https://doi.org/10.1007/s12272-020-01281-8

Promyo K, Iqbal F, Chaidee N, Chetsawang B (2020) Aluminum chloride-induced amyloid β accumulation and endoplasmic reticulum stress in rat brain are averted by melatonin. Food Chem Toxicol 146:111829. https://doi.org/10.1016/j.fct.2020.111829

Rahman MA, Shuvo AA, Bepari AK, Hasan Apu M, Shill MC, Hossain M, Uddin M, Islam MR, Bakshi MK, Hasan J, Rahman A, Rahman GMS, Reza HM (2022) Curcumin improves d-galactose and normal-aging associated memory impairment in mice: in vivo and in silico-based studies. PLoS ONE 17(6):e0270123. https://doi.org/10.1371/journal.pone.0270123

Rapaka D, Adiukwu PC, Bitra VR (2022) Experimentally induced animal models for cognitive dysfunction and Alzheimer's disease. Methods 9:101933. https://doi.org/10.1016/j.mex.2022.101933

Sano R, Reed JC (2013) ER stress-induced cell death mechanisms. Biochim Biophys Acta 1833 12:3460–3470. https://doi.org/10.1016/j.bbamcr.2013.06.028

Sha JY, Li JH, Zhou YD, Yang JY, Liu W, Jiang S, Wang YP, Zhang R, Di P, Li W (2021) The p53/p21/p16 and PI3K/Akt signaling pathways are involved in the ameliorative effects of maltol on

d-galactose-induced liver and kidney aging and injury. Phytother Res PTR 35(8):4411–4424. https://doi.org/10.1002/ptr.7142

Silva MVF, Loures CdMG, Alves LCV, de Souza LC, Borges KBG, Carvalho MdG (2019) Alzheimer's disease: risk factors and potentially protective measures. J Biomed Sci 26(1):33. https://doi.org/10.1186/s12929-019-0524-y

Singh NA, Bhardwaj V, Ravi C, Ramesh N, Mandal AKA, Khan ZA (2018) EGCG nanoparticles attenuate aluminum chloride induced neurobehavioral deficits, beta amyloid and tau pathology in a rat model of Alzheimer's disease. Front Aging Neurosci 10:244. https://doi.org/10.3389/fnagi.2018.00244

Song X, Zhao Z, Zhao Y, Jin Q, Li S (2022) Protective effects of *Bacillus coagulans* JA845 against d-galactose/AlCl$_{(3)}$-induced cognitive decline, oxidative stress and neuroinflammation. J Microbiol Biotechnol 32(2):212–219. https://doi.org/10.4014/jmb.2111.11031

Sprenkle NT, Sims SG, Sánchez CL, Meares GP (2017) Endoplasmic reticulum stress and inflammation in the central nervous system. Mol Neurodegener 12(1):42. https://doi.org/10.1186/s13024-017-0183-y

Sun L, Zhao Q, Xiao Y, Liu X, Li Y, Zhang J, Pan J, Zhang Z (2020) Trehalose targets Nrf2 signal to alleviate d-galactose induced aging and improve behavioral ability. Biochem Biophys Res Commun 521(1):113–119. https://doi.org/10.1016/j.bbrc.2019.10.088

Thibaudeau TA, Anderson RT, Smith DM (2018) A common mechanism of proteasome impairment by neurodegenerative disease-associated oligomers. Nat Commun 9(1):1097. https://doi.org/10.1038/s41467-018-03509-0

Uddin MS, Tewari D, Sharma G, Kabir MT, Barreto GE, Bin-Jumah MN, Perveen A, Abdel-Daim MM, Ashraf GM (2020) Molecular mechanisms of ER stress and UPR in the pathogenesis of Alzheimer's disease. Mol Neurobiol 57(7):2902–2919. https://doi.org/10.1007/s12035-020-01929-y

VerPlank JJS, Tyrkalska SD, Fleming A, Rubinsztein DC, Goldberg AL (2020) cGMP via PKG activates 26S proteasomes and enhances degradation of proteins, including ones that cause neurodegenerative diseases. Proc Natl Acad Sci USA 117(25):14220–14230. https://doi.org/10.1073/pnas.2003277117

Wang C, Cai X, Wang R, Zhai S, Zhang Y, Hu W, Zhang Y, Wang D (2020) Neuroprotective effects of verbascoside against Alzheimer's disease via the relief of endoplasmic reticulum stress in Aβ-exposed U251 cells and APP/PS1 mice. J Neuroinflammation 17(1):309. https://doi.org/10.1186/s12974-020-01976-1

Wei Y, Liu D, Zheng Y, Li H, Hao C, Ouyang W (2017) Protective effects of kinetin against aluminum chloride and d-galactose induced cognitive impairment and oxidative damage in mouse. Brain Res Bull 134:262–272. https://doi.org/10.1016/j.brainresbull.2017.08.014

Xu W, Zheng H, Fu Y, Gu Y, Zou H, Yuan Y, Gu J, Liu Z, Bian J (2022) Role of PI3K/Akt-mediated Nrf2/HO-1 signaling pathway in resveratrol alleviation of zearalenone-induced oxidative stress and apoptosis in TM4 cells. Toxins. https://doi.org/10.3390/toxins14110733

Yang X, Jia J, Ding L, Yu Z, Qu C (2021) The role of Nrf2 in d-galactose-induced cardiac aging in mice: involvement of oxidative stress. Gerontology 67(1):91–100. https://doi.org/10.1159/000510470

Yazdani A, Howidi B, Shi MZ, Tugarinov N, Khoja Z, Wintermark P (2021) Sildenafil improves hippocampal brain injuries and restores neuronal development after neonatal hypoxia–ischemia in male rat pups. Sci Rep 11(1):22046. https://doi.org/10.1038/s41598-021-01097-6

Yerbury JJ, Ooi L, Dillin A, Saunders DN, Hatters DM, Beart PM, Cashman NR, Wilson MR, Ecroyd H (2016) Walking the

tightrope: proteostasis and neurodegenerative disease. J Neurochem 137(4):489–505. https://doi.org/10.1111/jnc.13575

Yu L, Wc Di, Dong X, Li Z, Zhang Y, Xue Xd, Yl Xu, Zhang J, Xiao X, Js H, Liu Y, Yang Y, Hs W (2018) Melatonin protects diabetic heart against ischemia-reperfusion injury, role of membrane receptor-dependent cGMP-PKG activation. Biochim Biophys Acta (BBA) Mol Bas Dis 1864(2):563–578. https://doi.org/10.1016/j.bbadis.2017.11.023

Zhang B, Wang Y, Li H, Xiong R, Zhao Z, Chu X, Li Q, Sun S, Chen S (2016a) Neuroprotective effects of salidroside through PI3K/Akt pathway activation in Alzheimer's disease models. Drug Des Dev Ther 10:1335–1343. https://doi.org/10.2147/dddt.S99958

Zhang Y, Pi Z, Song F, Liu Z (2016b) Ginsenosides attenuate ᴅ-galactose- and AlCl3-inducedspatial memory impairment by restoring the dysfunction of the neurotransmitter systems in the rat model of Alzheimer's disease. J Ethnopharmacol 194:188–195. https://doi.org/10.1016/j.jep.2016.09.007

Zhang Y, Liu B, Chen X, Zhang N, Li G, Zhang LH, Tan LY (2017) Naringenin ameliorates behavioral dysfunction and neurological deficits in a ᴅ-galactose-induced aging mouse model through activation of PI3K/Akt/Nrf2 pathway. Rejuvenat Res 20(6):462–472. https://doi.org/10.1089/rej.2017.1960

Zheng Q, Huang T, Zhang L, Zhou Y, Luo H, Xu H, Wang X (2016) Dysregulation of ubiquitin-proteasome system in neurodegenerative diseases. Front Aging Neurosci 8:303. https://doi.org/10.3389/fnagi.2016.00303

Zhu G, Lee AS (2015) Role of the unfolded protein response, GRP78 and GRP94 in organ homeostasis. J Cell Physiol 230(7):1413–1420. https://doi.org/10.1002/jcp.24923

Publisher's Note Springer Nature remains neutral with regard to jurisdictional claims in published maps and institutional affiliations.